THE EFFECTIVENESS OF THE LIGHT-GAP METHOD FOR MONITORING SAW TENSIONING

by

PETER F. LISTER
BASc, University of British Columbia, 1989

A THESIS SUBMITTED IN PARTIAL FULFILLMENT OF
THE REQUIREMENTS FOR THE DEGREE OF
MASTER OF APPLIED SCIENCE

in

THE FACULTY OF GRADUATE STUDIES
(Department of Mechanical Engineering)

We accept this thesis as conforming
to the required standard

THE UNIVERSITY OF BRITISH COLUMBIA

March 1993

In presenting this thesis in partial fulfilment of the requirements for an advanced degree at the University of British Columbia, I agree that the Library shall make it freely available for reference and study. I further agree that permission for extensive copying of this thesis for scholarly purposes may be granted by the head of my department or by his or her representatives. It is understood that copying or publication of this thesis for financial gain shall not be allowed without my written permission.

(Signature)

Department of Mechanical Engineering

The University of British Columbia
Vancouver, Canada

Date March 31, 1993

DE-6 (2/88)

ABSTRACT

This thesis investigates the effectiveness of the light-gap method for evaluating the saw tensioning process. In particular, it examines the ability of the light-gap profile to indicate changes in saw natural frequency and stiffness caused by the tensioning stresses. The light-gap method for bandsaws is studied in detail. Many of the results are also expected to be applicable to circular saws. Although the light-gap method is a poor indicator of the details of the tensioning stress distribution, it does provide a good measure of changes in natural frequencies and stiffness caused by the tensioning process. In particular, when a bandsaw is tensioned to the traditional light-gap profile, the frequency and stiffness of the saw can be characterized by the curvature of the light-gap profile. Additionally, the light-gap method offers important practical advantages over other tensioning evaluation techniques. The light-gap method indicates local non-uniformities in the tensioning state, guides roll path location and indicates levelling defects. For these reasons, the light-gap method is confirmed to be a highly effective and rational way of monitoring the saw tensioning process.

TABLE OF CONTENTS

LIST OF TABLES

LIST OF FIGURES

NOMENCLATURE

a	=	length of the rectangular plate in the x-direction
A,B	=	parameters for $w_o(y)$
A_d,C_d	=	constants for W_{sym} and W_{skew}
A_f,C_f	=	constants for w_{lat} and w_{tor}
A^*,B^*	=	parameter for the δ/h calculation
A_n	=	magnitude of the nth term of the tensioning stress function
b	=	width of the rectangular plate in the y-direction
b_n	=	magnitude of the nth term of $w_n(y)$
C	=	applied curvature parameter for the δ/h calculation
D	=	$Eh^3/12(1-\nu^2)$, plate stiffness parameter
E	=	Young's modulus for the plate material
$F(x)$	=	line load used in stiffness calculation
F_t	=	magnitude of $F(x)$, in force per unit length
h	=	thickness of the rectangular plate
K	=	"cutting stiffness" of the plate
n	=	term number for the tensioning stress function
R	=	applied radius of curvature used in the light-gap calculation
$W(y)$	=	approximate displacement function used in the stiffness calculation
W_{skew}	=	approximate displacement function for the skew-symmetric part of $W(y)$

W_{sym} = approximate displacement function for the symmetric part of W(y)

$w(y)$ = lateral displacement profile of the rectangular plate model

$w_o(y)$ = component of w(y) associated with the stress-free plate

$\Delta w(y)$ = component of w(y) associated with the tensioning stresses

$w_n(y)$ = n^{th} component of $\Delta w(y)$

w_{lat} = approximate mode shape for the first lateral frequency

w_{tor} = approximate mode shape for the first torsional frequency

x, y, z = coordinates for the rectangular plate calculations

α_n = stress parameter for the δ/h calculation

β^4 = $3(1-\nu^2)/(R^2h^2)$

δ = size of the light-gap profile

ε = parameter for the δ/h calculation

γ = constant for the δ/h calculation

κ = curvature of w(y)

λ_{11} = frequency parameter for the first lateral frequency

λ_{12} = frequency parameter for the first torsional frequency

ν = Poisson's ratio for the plate material

ω_{lat} = natural frequency for the first lateral mode

ω_{tor} = natural frequency for the first torsional mode

ρ = density of the saw plate material

$\sigma_x(y)$ = residual tensioning stress distribution

ξ = a/b, length to width ratio of the rectangular plate

ACKNOWLEDGEMENT

This thesis is dedicated to my parents, Jim and Christine, and my sister, Debby. Your love and encouragement have made this possible.

Also, I would like to thank the many people who have had an influence on this work. In particular, I would like to thank Dr. Gary Schajer, Dr. George Shipley, Dr. Ricardo Foschi, Dr. Eb Kirbach, John Taylor, Bruce Lehmann and Jan Aune. Thanks to all.

The work reported here was supported by the B.C. Science Council and MacMillian Bloedel Ltd. through the GREAT program and by the Natural Sciences and Engineering Research Council of Canada (NSERC).

1.0 INTRODUCTION

1.1 Background and motivation

Sawmills use band and circular saws to cut raw logs into saleable lumber. Each time a saw cut is made, a certain amount of solid wood is lost as sawdust. The amount of sawdust waste produced annually is considerable. In British Columbia alone about fifty million cubic meters of raw logs are processed each year [1]. Of this amount, approximately 10% of the wood is wasted to sawdust during the cutting process. This large amount of wasted wood presents a considerable economic and environmental cost to the forest industry.

To reduce the amount of wood lost to sawdust, "thin-kerf" saws are being adopted by industry. These thinner saws produce less sawdust because the width of the saw cut is reduced. Even small reductions in saw thickness can result in a considerable reduction in sawdust and an even larger increase in lumber recovery [2]. For example, studies by the U.S. Forest Service have shown that a 0.012 in. reduction in the saw kerf of a typical 4/4 (1 inch board) mill can increase lumber recovery by 1 percent [3]. Because raw logs account for 75-80 percent of the total production cost for many sawmills, even small increases in lumber recovery can represent a considerable increase in revenue [4].

Reductions in saw kerf are limited by the reduced cutting accuracy and stability associated with thinner saw blades. Thinner saws are less stiff than their thicker predecessors and are less able to resist the lateral forces generated during cutting. Large lumber dimension variations can result when the lateral forces cause the saw blade to deviate from the desired path. Poor dynamic behavior caused by the critical speed phenomena can also occur as saw thickness is reduced [5]. A saw operating at or near its critical speed will often snake slowly

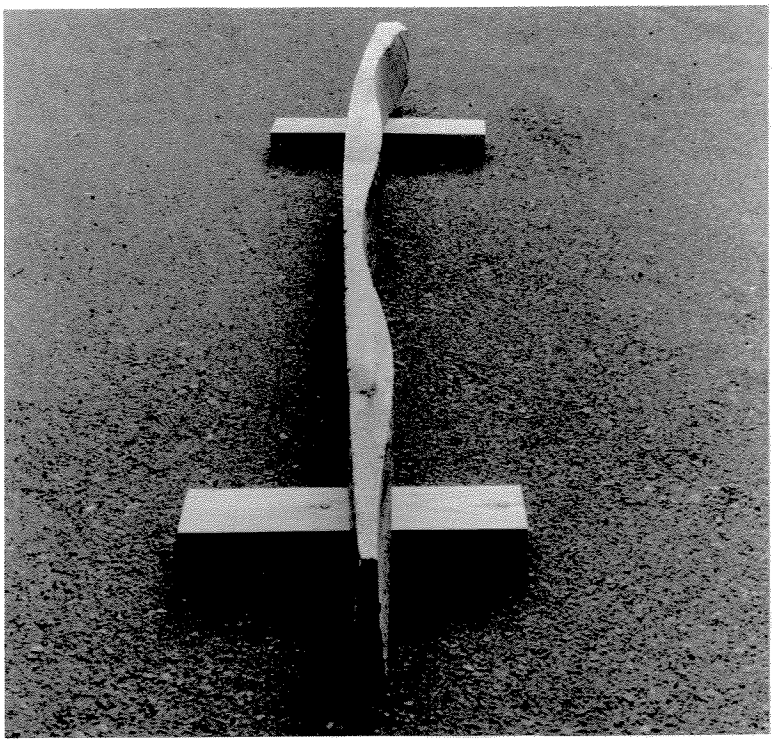

Figure 1.1 Wavy saw cut caused by critical speed instability of a circular saw.

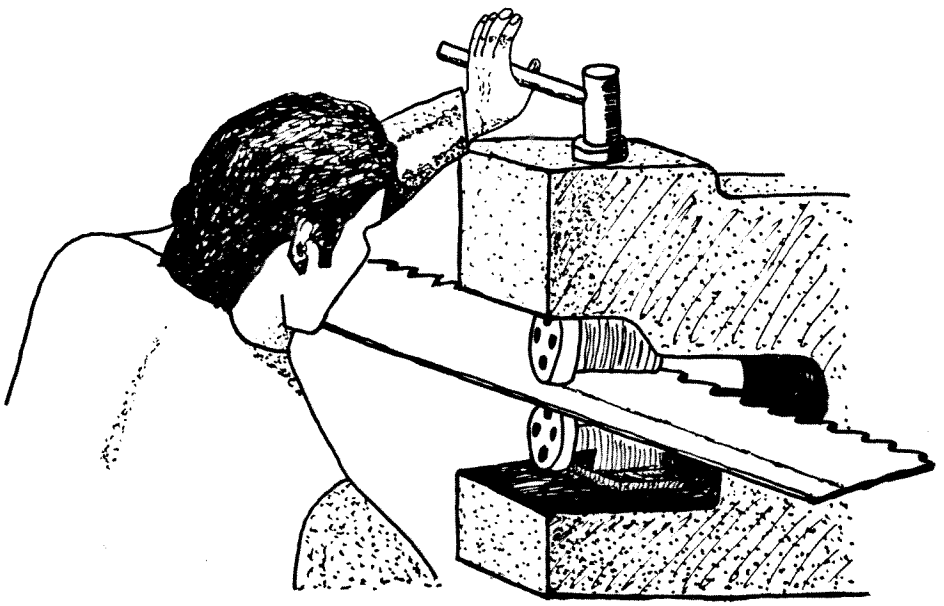

Figure 1.2 Typical roll tensioning machine for bandsaw blades.

from side-to-side and cut grossly inaccurate lumber. Figure 1.1 shows a typical example of a wavy saw cut produced by a circular saw suffering from critical speed instability.

"Tensioning" is a process used to enhance the stiffness and dynamic stability of thin-kerf saws [6,7]. The process involves inducing residual stresses into a saw plate, typically by mechanical means such as hammering or rolling [8,9]. Roll tensioning is the preferred method because it is faster and gives more uniform results than hammering. Other tensioning methods, such as shot peening, thermal tensioning and laser tensioning, have also been investigated but are not generally used by industry [10,11,12].

Figure 1.2 shows a typical roll tensioning machine used for tensioning bandsaws. Similar machines are also used for circular saws. Roll tensioning machines have two narrow crowned rollers which squeeze a small portion of the saw plate. One or both of the rollers is driven so that the saw slowly moves and a narrow squeezed path is created in the longitudinal direction for bandsaws or in the circumferential direction for circular saws. The deformations caused by rolling induce residual stresses into the saw plate. When these stresses are induced in a favorable manner, the lateral stiffness of the saw increases. This stiffness increase improves the accuracy of the saw cut [13]. Favorable tensioning stresses also improve the dynamic stability of a saw because they raise the natural frequencies which control critical speed [14]. Figure 1.3 schematically illustrates the relationship between the saw tensioning process, residual stresses and cutting accuracy.

Achieving effective results from the tensioning process requires a method of evaluating the effect of the residual stresses. A number of different non-destructive methods are available for measuring the residual stresses directly [15]. In general, these methods have been developed for experimental stress analysis and are either too costly, too time consuming or too awkward for day-to-day use.

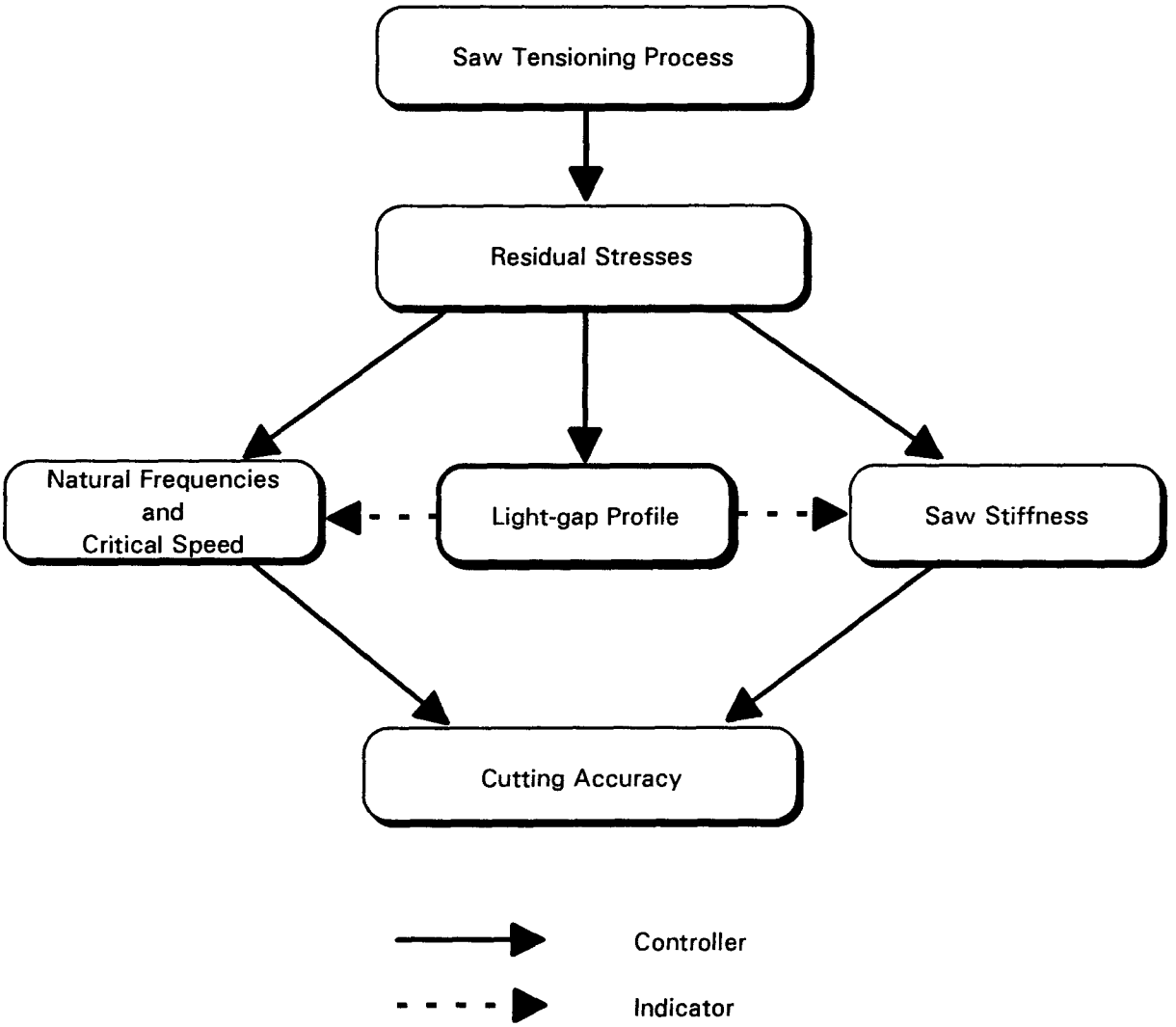

Figure 1.3 Schematic relationship between the saw tensioning process, cutting accuracy and light-gap profile.

The most common industrial technique for monitoring the saw tensioning process is the "light-gap" method [16]. Very rarely, natural frequency measurements are also used [17]. Figure 1.3 schematically shows how both the light-gap and the natural frequencies are controlled by the residual stresses induced by the tensioning process.

Previous studies of saw tensioning have focused on the relationships between the tensioning stresses and frequencies, and the tensioning stresses and light-gap profile. The frequency relationships have been studied in detail for circular saws [6,14,18,19], but have been less widely studied for bandsaws [20]. The light-gap relationships have not been well studied. Foschi [21] studied the relationship between residual stresses and the light-gap profile for bandsaws. Similar studies for circular saws have not been reported in the literature.

The relationships developed by Foschi show that the light-gap method is a rather poor indicator of the details of the tensioning stress distribution. Because of this feature, the light-gap method has been criticized as being a poor indicator of the tensioning state of a saw. However in practice, the light-gap method is used to indicate changes in saw stiffness and natural frequencies caused by the tensioning stresses. This is indicated in Figure 1.3 by the dashed lines. The effectiveness of the light-gap method for indicating these changes in saw stiffness and frequencies has not been previously studied.

1.2 The light-gap method

The light-gap method is used for both band and circular saws. The procedure is essentially the same for both types of saws, with a few minor differences.

Figure 1.4 illustrates the light-gap method for a bandsaw. The procedure involves inducing a curvature along the length of the saw blade which in turn induces a corresponding curvature across the saw width. The shape and size of the lateral displacement across the saw width depends on the local tensioning stresses and can be used to monitor the tensioning process. In practice, the lateral displacement is evaluated by placing a curved tension gauge across the width of the plate as shown in the figure. The tension gauge has a shallow circular profile with an empirically chosen curvature. The gauge contacts the saw at two or more "high points". The resulting clearance between the saw and the gauge is called the "light-gap" and is used to monitor the tensioning process.

Figure 1.5 illustrates the light-gap method for a circular saw. The procedure is basically the same as for a bandsaw except the induced curvature is applied by supporting the saw at two points across a diameter and letting the saw sag under its own weight. The lateral displacement is then evaluated by placing a tension gauge across a perpendicular radius.

Both the size and shape of the lateral displacement profile are known to be important indicators of the tensioning state for both band and circular saws. The size of the lateral displacement is important because it indicates the overall amount of tensioning. The shape is important because it is used to guide the distribution of the tensioning stresses.

1.3 Objectives and scope

The objective of this study is to investigate the effectiveness of the light-gap method for evaluating the tensioning state of a saw. The light-gap method for a bandsaw is studied in detail because the mathematics are simpler than for a circular saw and an exact solution for the lateral displacement is available. Thus, the characteristics and significance of the solution

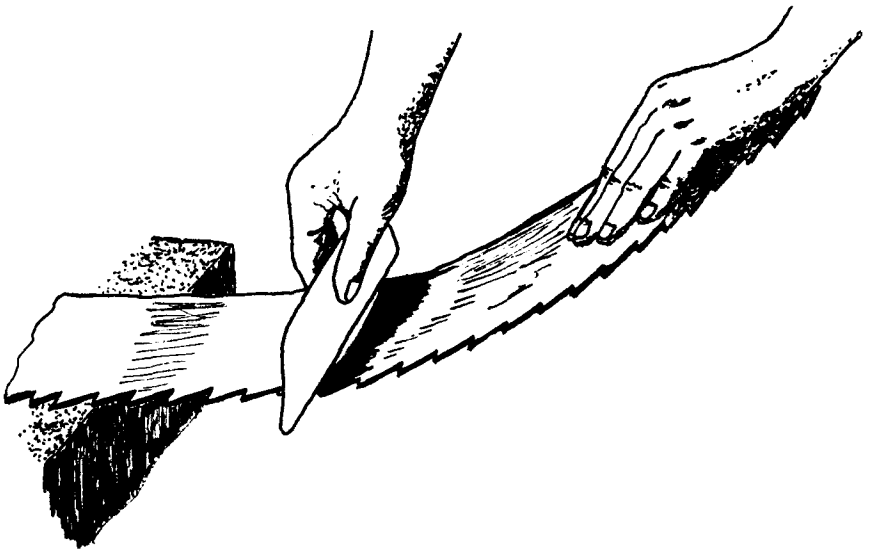

Figure 1.4 The light-gap method for a bandsaw.

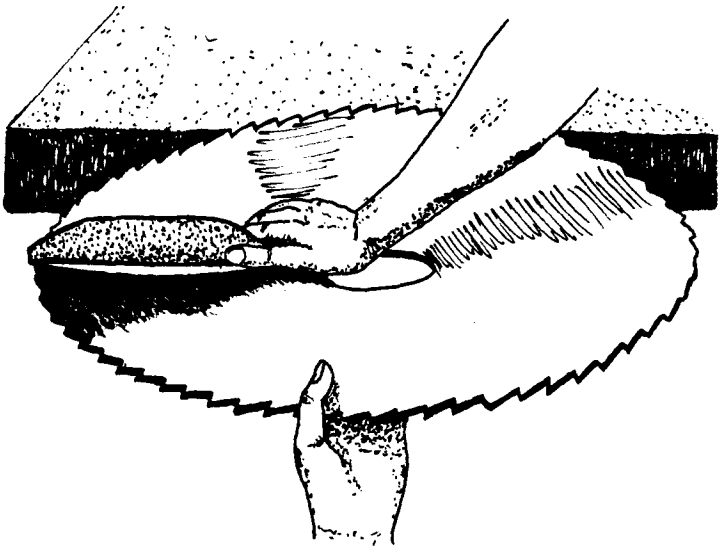

Figure 1.5 The light-gap method for a circular saw.

can be interpreted more clearly and simply. Although the results obtained apply specifically to bandsaws, the general features are also expected to apply to circular saws.

A discussion of the light-gap method for bandsaws is presented in Chapters 2 to 7.

In Chapter 2, a rectangular plate model representing a bandsaw is presented. The stresses induced by roll tensioning a bandsaw are briefly discussed and relationships between the tensioning stresses and lateral displacement, natural frequency and stiffness are given. These relationships are used in Chapter 3 to show how roll path position influences bandsaw lateral displacement, torsional frequency and stiffness.

Chapter 4 describes the practical use of the light-gap method as a guide for the saw tensioning process. Empirically developed rules-of-thumb used by sawfilers to obtain the desired light-gap profile are discussed and are illustrated with an example case of bandsaw tensioning. Some additional factors concerning the practical use of the light-gap method are discussed in Chapter 5.

In Chapter 6, the effectiveness of the light-gap method is investigated. In particular, the significance of the size and shape of the light-gap profile in terms of bandsaw frequency and stiffness is studied.

Chapter 7 discusses some of the more important practical advantages and limitations of the light-gap method. Some simple ways of improving the results of the light-gap method are presented.

2.0 GENERAL BANDSAW RELATIONSHIPS

2.1 Chapter overview

In this chapter, a rectangular plate model representing a bandsaw blade is introduced and is used to illustrate the influence of tensioning stresses on the lateral displacement, frequency and stiffness of a saw.

The residual tensioning stresses resulting from roll tensioning a bandsaw are briefly presented and the relationships between lateral displacement and stress, frequency and stress, and stiffness and stress are given.

Finally, approximate simplified relationships are developed and are used to compare the influence of tensioning stresses on saw lateral displacement, frequency and stiffness.

2.2 Stresses induced by roll tensioning bandsaw blades

Bandsaws are commonly tensioned using a roll tensioning machine of the type illustrated in Figure 1.2. A part of the saw is squeezed between two crowned rollers creating a narrow rolled path along the length of the saw surface as the rollers turn. The part of the saw blade within the roll path becomes slightly thinner and the displaced material spreads longitudinally and laterally. The lateral spreading has a negligible influence on the tensioning stresses because the saw plate is free to expand laterally. The longitudinal spreading, however, is resisted by the surrounding plate material. As a result, compressive stresses are induced within the roller path and tensile stresses are induced in the remainder of the plate.

Figure 2.1 shows a typical stress distribution caused by rolling a rectangular plate of width b along its centreline, y=0. Large compressive stresses occur within the roller path which are balanced by tensile stresses in the adjacent regions. These stresses are self-equilibrating because no external in-plane loads are applied. The magnitude of the compressive stress depends on the force applied to the rollers, and has a maximum of about 40% of the yield stress of the material [18]. This limit occurs when the compressive stresses become large enough to inhibit any additional longitudinal deformations in the roll path which would further increase the compressive stresses. Once the limiting compressive stress is reached, any additional rolling along the same roller path simply makes the saw plate wider and provides little additional tensioning effect.

Because the maximum stress level within a single roll path is limited, the desired level of tensioning can most effectively be achieved by using a number of roll tensioning paths. The resulting stress distribution is the superposition of the stress distributions resulting from each separate roll path.

Typically the back edge of a bandsaw blade is rolled slightly more than the front in order to induce a very small curvature along the back of the saw. This curvature, called "backcrown", helps to stiffen the front edge of the saw when it is mounted on a bandmill. The component of the tensioning stresses associated with backcrown is non-symmetric with respect to the saw centreline. However, these non-symmetric stresses are usually quite small and can be neglected for the types of calculations considered here. The remaining tensioning stresses are reasonably symmetric and can be approximated by a Fourier cosine series,

$$\sigma_x(y) \approx \sum_n A_n \cos\frac{2n\pi y}{b} \qquad n = 1,2,3,... \tag{2.1}$$

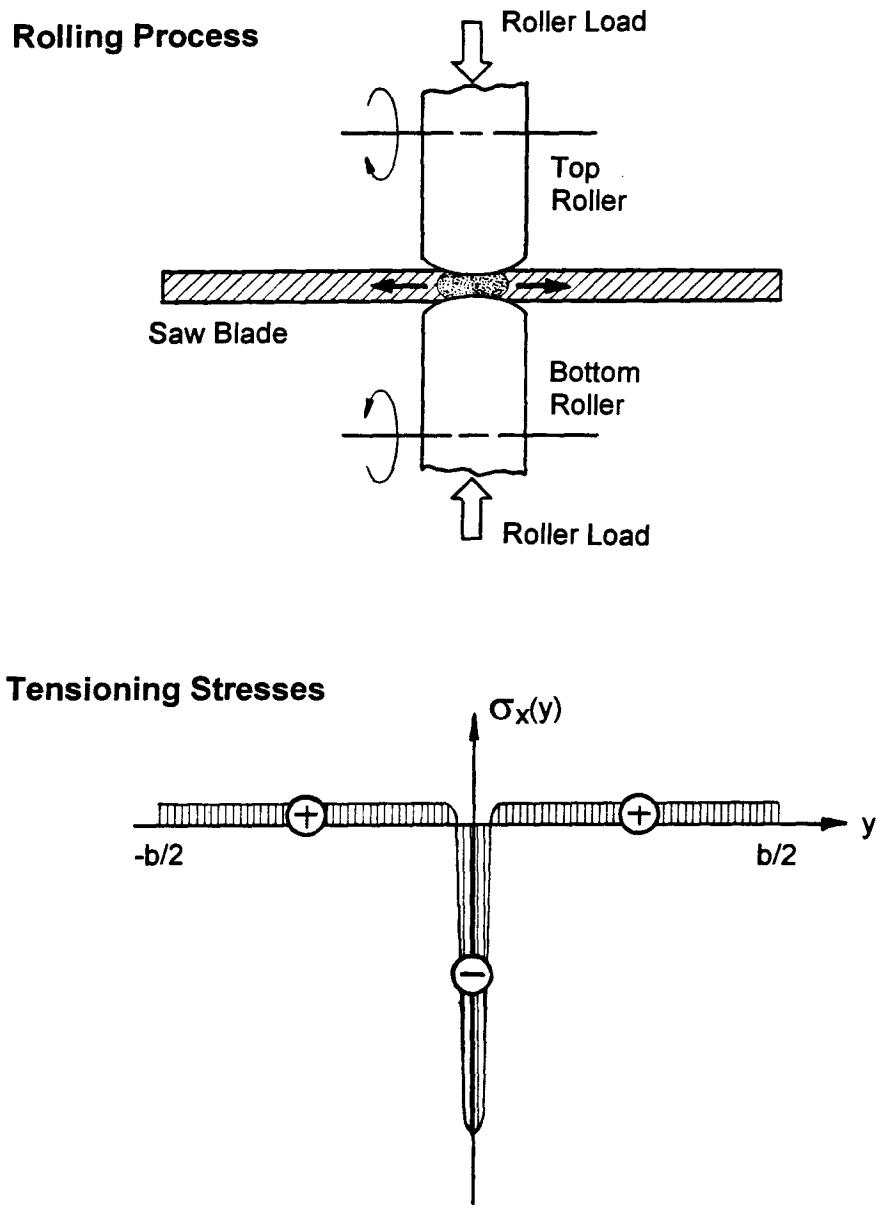

Figure 2.1 The bandsaw roll tensioning process and resulting residual stress distribution.

where b is the width of the plate in the y-direction and y is measured from the plate centreline. The magnitude of each term in Equation (2.1) is found from

$$A_n = \frac{4}{b}\int_0^{b/2}\sigma_x(y)\cos\frac{2n\pi y}{b}dy \tag{2.2}$$

where $\sigma_x(y)$ is the actual stress distribution.

2.3 Relationship between lateral displacement and stress

Figure 2.2 shows a rectangular plate model that can be used to study the relationship between the tensioning stresses and the lateral displacement of a bandsaw. The plate shown has width b in the transverse ("y") direction and is considered to be long in the longitudinal ("x") direction. It contains in-plane tensioning stresses and is initially flat. When the plate is bent to a radius R along its length, a lateral displacement is induced along the transverse direction. The shape and magnitude of the lateral displacement profile depends on the local tensioning stresses and can be used to monitor the tensioning state of the saw. Both the size and the shape of the lateral displacement profile are important indicators of the tensioning state of the saw.

An exact solution for the lateral displacement, w(y), of the bent plate in Figure 2.2 is described by Foschi [21]. The governing equation is

$$\frac{d^4w}{dy^4} + 4\beta^4 w = 4\beta^4\frac{R}{E}\sigma_x(y) \qquad \beta^4 = \frac{3(1-\nu^2)}{R^2h^2} \tag{2.3}$$

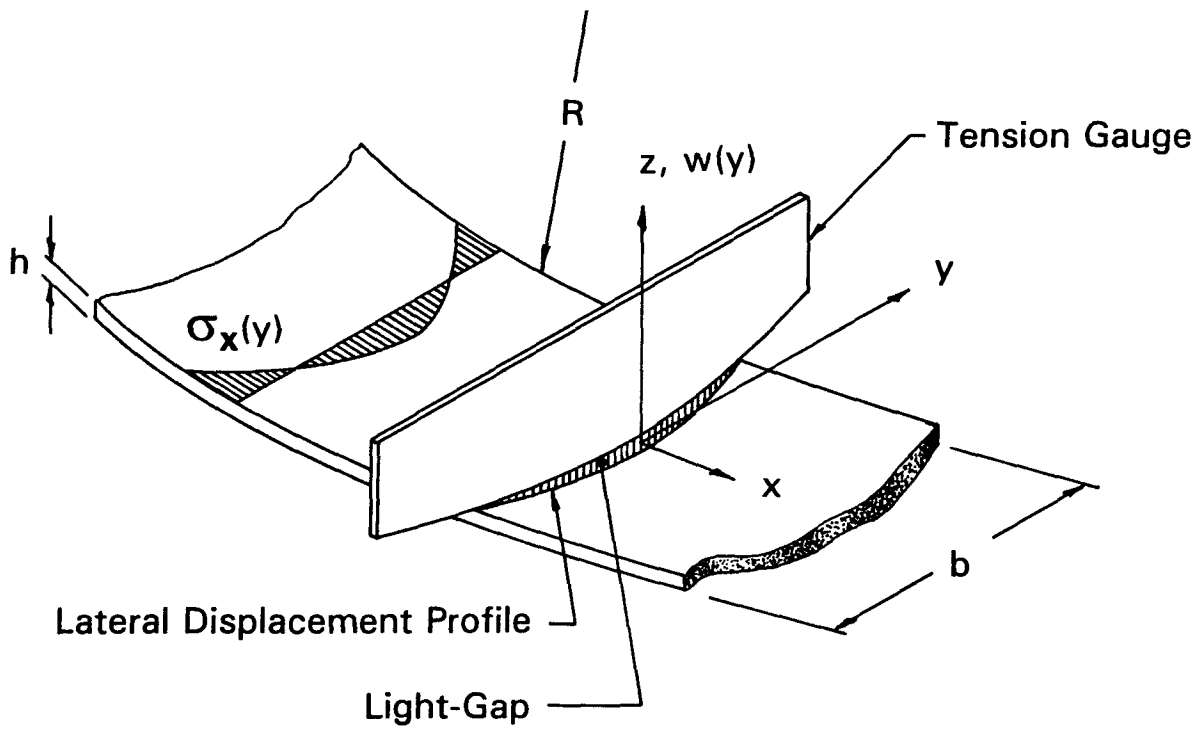

Figure 2.2 Rectangular plate model used for the light-gap calculations.

Table 2.1 Rectangular plate dimensions and parameters used in the examples.

Plate width, b	=	0.254 m
Plate span, a	=	0.508 m
Thickness, h	=	0.002 m
Young's Modulus, E	=	210 GPa
Poisson's Ratio, ν	=	0.3
Density, ρ	=	7850 kg/m^3

and the boundary conditions at y = ± b/2 are

$$\frac{d^3w}{dy^3} = 0 \qquad \frac{d^2w}{dy^2} = -\frac{\nu}{R} \tag{2.4}$$

A detailed discussion of the governing equation and boundary conditions is given by Conway and Nickola [22] for the case when no tensioning stresses are present.

When tensioning stresses are present the lateral displacement, w(y), satisfying the governing equation and boundary conditions is the sum of two parts

$$w(y) = w_o(y) + \Delta w(y) \tag{2.5}$$

The first part, $w_O(y)$, is the displacement of the stress-free plate and the second part, $\Delta w(y)$, is the additional displacement due to the tensioning stresses.

The displacement of the stress-free plate is given by

$$w_o(y) = A\cosh\beta y\cos\beta y + B\sinh\beta y\sin\beta y \tag{2.6}$$

where

$$A, B = -\frac{\nu}{R\beta^2}\frac{\sinh\frac{\beta b}{2}\cos\frac{\beta b}{2} \mp \cosh\frac{\beta b}{2}\sin\frac{\beta b}{2}}{\sinh\beta b + \sin\beta b} \tag{2.7}$$

Figure 2.3a shows the displaced shape, $w_O(y)$, described by Equations (2.6) and (2.7) for a rectangular plate having dimensions given in Table 2.1. Only half of the plate is shown

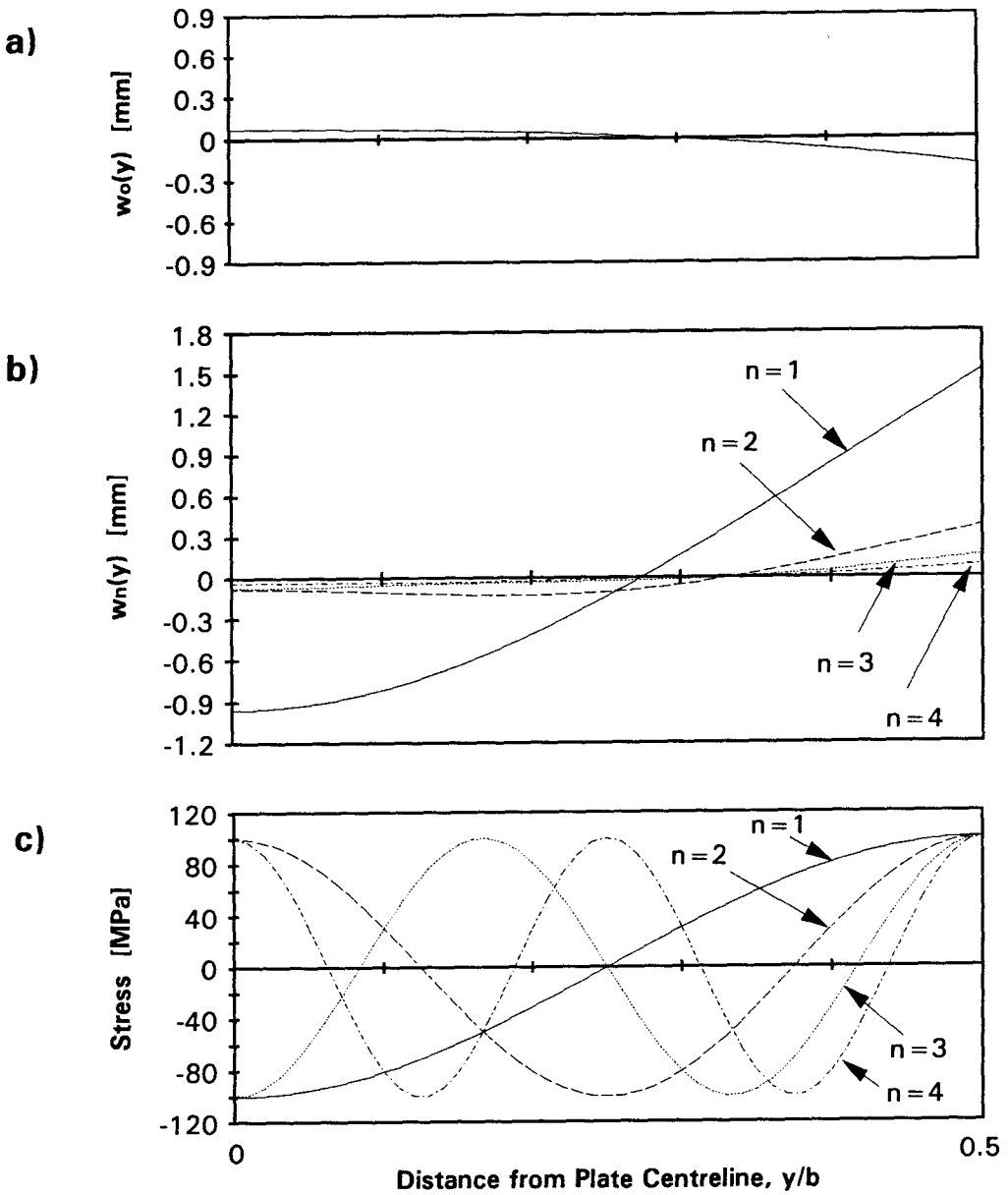

Figure 2.3 Lateral displacement components for a bandsaw.
a) Component of lateral displacement associated with the stress-free plate.
b) Components of lateral displacement associated with each tensioning stress term shown in c).

because the displacement is symmetric with respect to the plate centreline, y/b=0. The displaced shape describes an anticlastic surface because the lateral displacement is convex when the applied curvature in the x-direction is concave.

The change in displacement caused by the tensioning stresses, $\Delta w(y)$, is the sum of the displacement curves, $w_n(y)$, associated with each term of the stress series in Equation (2.1). The change in displacement is given by

$$\Delta w(y) = \sum_n w_n(y) \qquad n = 1,2,3,\ldots \tag{2.8}$$

where

$$w_n(y) = b_n \frac{R}{E}\left[\cos\frac{2n\pi y}{b} - (-1)^n \frac{R}{\nu}\left(\frac{2n\pi}{b}\right)^2 w_o(y)\right] \tag{2.9}$$

$$b_n = \frac{A_n}{1+4\left[\frac{n\pi}{\beta b}\right]^4} \tag{2.10}$$

and A_n is the magnitude of the nth stress term in Equation (2.1).

Figure 2.3b shows the individual displacement curves, $w_n(y)$, associated with each of the first four terms of the stress series in Equation (2.1). Again, the plate has dimensions given in Table 2.1 and only half of the plate is shown because of symmetry. The sign and magnitude of each stress term has been chosen so that the stresses are all the same size and are tensile at the plate edge as shown in Figure 2.3c. The tensile edge stresses result in $w_n(y)$ curves which have a generally concave shape when the applied curvature in the longitudinal direction is also concave.

Figure 2.3b shows that the $w_n(y)$ curve associated with the n=1 stress term has the largest size and therefore has the largest influence on the lateral displacement. As the value of n increases, the size of the $w_n(y)$ curves decrease rapidly. For large values of n, the $w_n(y)$ curves become very small and have a negligible influence on the lateral displacement of the saw, even though the associated stresses may be quite large.

The shape of the lateral displacement profile of a bandsaw can be more easily seen by looking at the curvature across the width of the saw. The curvature, κ, is given by the second derivative of Equation (2.5),

$$\kappa = w''(y) = w_0''(y) + \Delta w''(y) \tag{2.11}$$

where

$$w_0''(y) = 2B\beta^2 \cosh\beta b \cos\beta b - 2A\beta^2 \sinh\beta b \sin\beta b \tag{2.12}$$

$$\Delta w''(y) = \sum_n w_n''(y) \qquad n = 1,2,3,\ldots \tag{2.13}$$

and

$$w_n''(y) = -b_n \frac{R}{E}\left(\frac{2n\pi}{b}\right)^2 \left[\cos\frac{2n\pi y}{b} + (-1)^n \frac{R}{\nu} w_o''(y)\right] \tag{2.14}$$

Figure 2.4a shows the curvature of the stress-free component of displacement shown in Figure 2.3a. The curvature is described by Equation (2.12) and is shown in the figure for half of the plate width. The curvature of the stress-free plate is positive and increases towards the plate edges because the shape of $w_o(y)$ becomes increasingly convex near the outside of the plate.

Figure 2.4b shows the curvatures of the four $w_n(y)$ displacement components shown in Figure 2.3b. The curvatures are described by Equation (2.14) for each of the stress terms reproduced

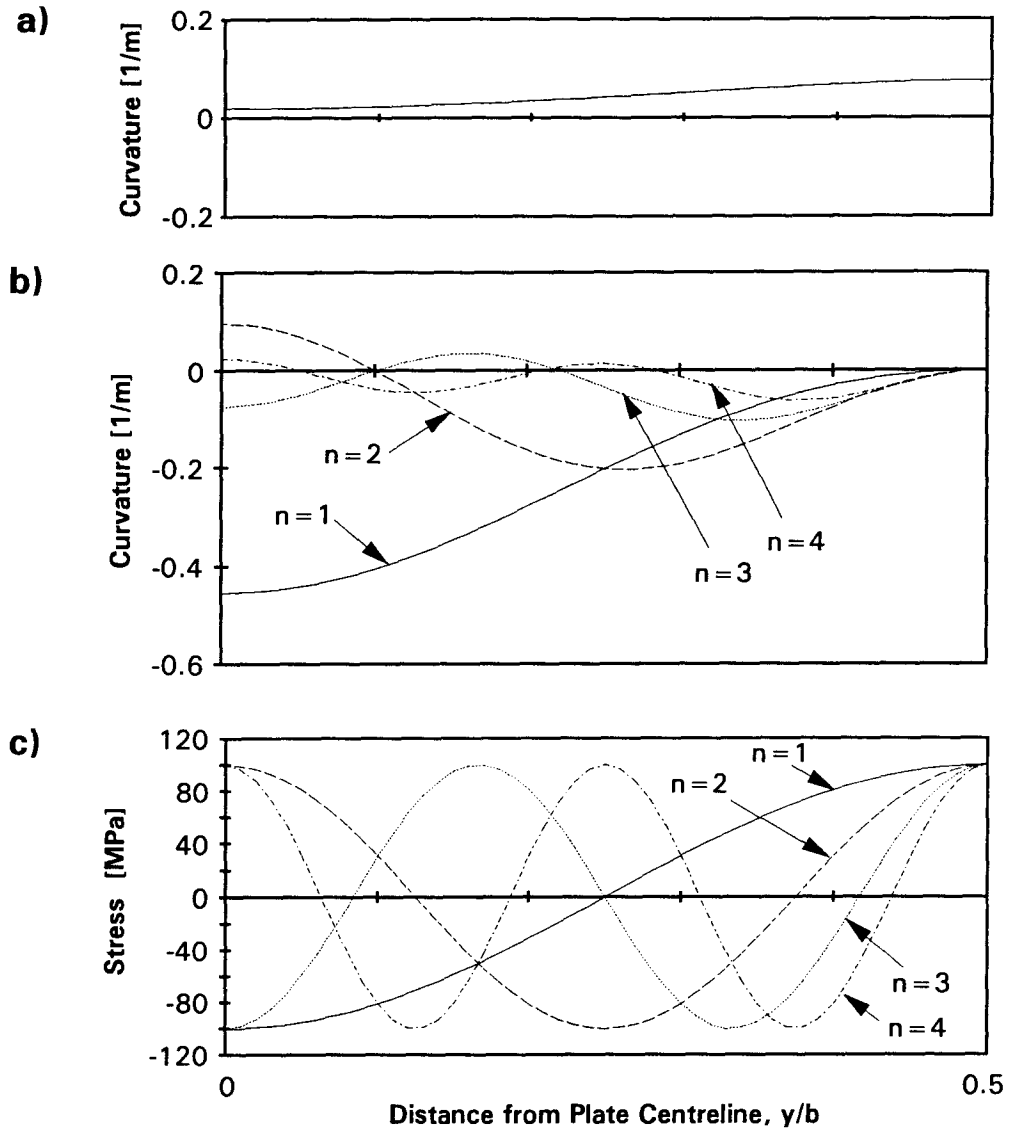

Figure 2.4 Curvatures of the lateral displacements shown in Figure 2.3.
a) Curvature of the stress-free component, $w_o(y)$.
b) Curvatures of the stress-related components, $w_n(y)$.
c) Tensioning stresses repeated from Figure 2.3.

in Part (c) of the figure. The curvatures of the $w_n(y)$ components are different from one another indicating that each $w_n(y)$ curve has a unique shape. Each curve has negative values of curvature corresponding to the compressive regions in each stress term. The negative areas of curvature indicate concave shaped displacements and occur because the compressive stresses tend to push the plate out of plane when it is bent along its length. The areas of the plate which contain tensile stresses have a less concave shape because tensile stresses tend to pull the plate back into plane.

Because each of the $w_n(y)$ curves have a unique shape, the shape of the lateral displacement profile, w(y), of a tensioned bandsaw depends on the relative amount of each of the first few $w_n(y)$ components. The first few stress terms in Equation (2.1) associated with these displacement components describe a slowly varying "average" of the actual tensioning stress distribution. The higher stress terms describe the details of the tensioning stresses, but hardly influence the lateral displacement profile. In practice this means that stress distributions which have the same "average" produce similar light-gap profiles, even though the details of the stress distributions may be quite different.

2.4 Relationship between natural frequency and stress

Natural frequency measurements are sometimes used to monitor the saw tensioning process because the stresses induced by tensioning affect the frequencies associated with certain vibration modes. For circular saws, the vibration mode which controls the lowest critical speed of a saw is typically monitored. Although the frequency measurement method is generally used only on circular saws, it could also be used for bandsaws if the saw blade were supported in a suitable manner.

The effectiveness of the frequency measurement method depends on which natural frequencies are monitored. Theoretically, a rectangular plate has an infinite number of natural frequencies. However in practice, only the lower frequencies are of interest because these have the largest influence on sawing performance. The two lowest frequencies are for the first lateral and first torsional modes illustrated in Figure 2.5 [23]. The influence of tensioning stresses on the frequencies of these two modes is investigated in this section.

The rectangular plate shown in Figure 2.5 provides a simple model for studying the relationships between the tensioning stresses and the natural frequencies of an unstrained bandsaw blade. The plate has width b, length a, and thickness h. It is simply-supported along the x=0 and x=a edges and free on the other two edges. The tensioning stresses are assumed to be symmetric and described by Equation (2.1).

In general, a simple exact solution for the frequencies of the rectangular plate model is not possible when tensioning stresses are present. However, an upper-bound estimate of the lower frequencies can be obtained using Rayleigh's method [24] and appropriate mode shape functions. The accuracy of this method depends on the similarity of the assumed shape function and the actual mode shape. Because the general nature of the solution is of primary interest here, the simplest admissible shape functions are used in this analysis. For the first lateral and first torsional modes, the chosen approximate shape functions are

$$w_{lat}(x,y) = A_f \, sin\frac{\pi x}{a} \tag{2.15}$$

and

$$w_{tor}(x,y) = C_f \, y \, sin\frac{\pi x}{a} \tag{2.16}$$

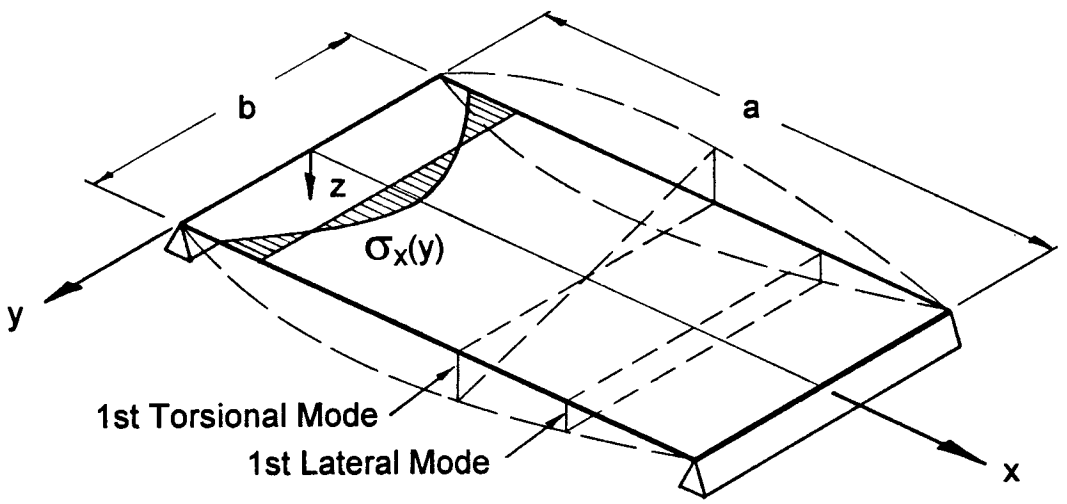

Figure 2.5 Rectangular plate model for the natural frequency calculations.

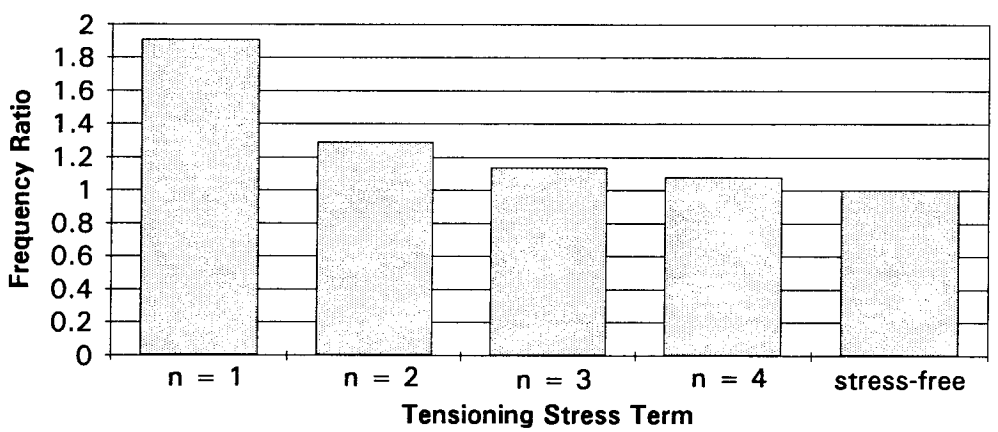

Figure 2.6 Influence of the individual tensioning stress terms on torsional frequency ratio when the tensioning stresses are as shown in Figure 2.3c.

where A_f and C_f are constants.

Following the procedure for Rayleigh's method, (2.15) and (2.16) can be used to calculate the maximum potential and kinetic energies of the vibrating system. Equating the potential and kinetic energies gives the following estimates for the frequencies of the first lateral and first torsional modes

$$\omega_{lat}^2 = \frac{D}{a^4 \rho h}\left[\pi^4 + \frac{2\pi^2 a^2 h}{D\xi}\int_0^{b/2}\sigma_x(y)dy\right] \tag{2.17}$$

and

$$\omega_{tor}^2 = \frac{D}{a^4 \rho h}\left[\pi^4 + 24\pi^2(1-\nu)\xi^2 + \frac{24\pi^2 a^2 h}{Db^3}\int_0^{b/2} y^2\sigma_x(y)dy\right] \tag{2.18}$$

where the integral terms are associated with the tensioning stresses.

The integral term in Equation (2.17) is identically zero because the tensioning stresses given by Equation (2.1) are self-equilibrating. Therefore, the first lateral frequency reduces to

$$\omega_{lat} = \frac{\lambda_{11}}{a^2}\sqrt{\frac{D}{\rho h}} \tag{2.19}$$

where

$$\lambda_{11} = \pi^2 \approx 9.87 \tag{2.20}$$

Equations (2.19) and (2.20) show that the tensioning stresses have no effect on the first lateral frequency. This result occurs because the mode shape has a constant displacement along the

width of the plate. Consequently, the first lateral frequency is not an effective indicator of the tensioning stresses.

When the tensioning stresses are given by Equation (2.1), the integral term in Equation (2.17) is easily evaluated and the first torsional frequency is

$$\omega_{tor} = \frac{\lambda_{12}}{a^2}\sqrt{\frac{D}{\rho h}} \tag{2.21}$$

where

$$\lambda_{12} = \sqrt{\pi^4 + 24\pi^2(1-\nu)\xi^2 + \frac{6a^2h}{D}\sum_n \frac{(-1)^n}{n^2}A_n} \qquad n = 1,2,3,... \tag{2.22}$$

The summation term in Equation (2.22) is the change in the first torsional frequency caused by the tensioning stresses. This term is sufficiently large to enable the first torsional frequency to be used successfully to infer the tensioning state.

Figure 2.6 shows the effect of tensioning stresses on the first torsional frequency for a rectangular plate with dimensions given in Table 2.1. The frequency of the stress-free plate, 53.2 Hz, is used to normalize the frequencies of the plate containing the example tensioning stress distributions. Each of the example stress distributions have the same peak value and are the same as the stresses shown in Figure 2.3c. The stresses are tensile along the plate edges, $y=\pm b/2$, which cause the frequency of the plate to increase. However, the amount of the increase diminishes as the value of n in Equation (2.1) increases.

Figure 2.6 shows that, in a manner similar to the lateral displacement, the torsional frequency is most influenced by the lowest terms in Equation (2.1). These terms describe a slowly

varying "average" of the actual stress distribution. Additionally, the summation term in Equation (2.22) shows that the torsional frequency depends only on the cumulative effect of the stress terms and not on the size of each term individually.

2.5 Relationships between stiffness and stress

Figure 2.7a shows a rectangular plate with the same dimensions, support conditions and tensioning stresses as that shown in Figure 2.5. A line load, F(x), is distributed along one free edge. The loaded plate approximately represents an unstrained bandsaw blade subjected to a lateral cutting force acting on the saw teeth. It provides a model for investigating the influence of tensioning stresses on the "cutting stiffness" of the plate.

The cutting stiffness of the plate is chosen in a manner which provides a measure of the ability of the saw plate to resist lateral cutting forces. Therefore, an increase in a plate's stiffness would be expected to result in improved cutting accuracy. For mathematical simplicity, the lateral cutting force, F(x), acting on the plate edge, y=b/2, is approximated as

$$F(x) = F_t \sin\frac{\pi x}{a} \tag{2.23}$$

The cutting stiffness, K, is defined as

$$K = \frac{\int_o^a F(x)}{W(x = a/2, y = b/2)} \tag{2.24}$$

where W(a/2, b/2) is the maximum displacement of the plate.

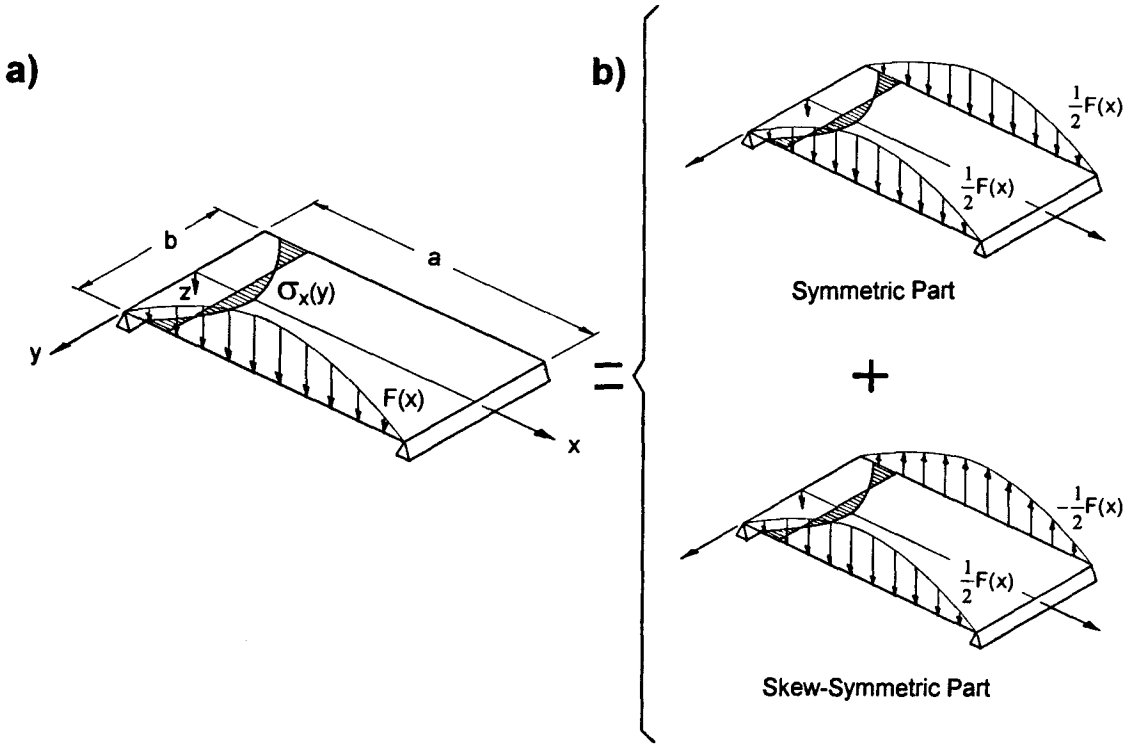

Figure 2.7 Rectangular plate model for the stiffness calculation.

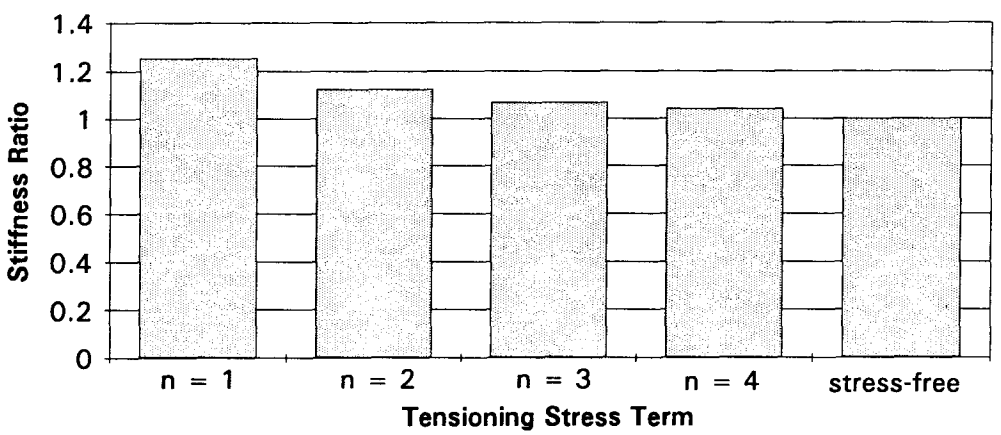

Figure 2.8 Influence of the individual tensioning stress terms on stiffness ratio when the tensioning stresses are as shown in Figure 2.3c.

The deflection of the plate in Figure 2.7a may be found by superposing the displacements of the symmetric and skew-symmetric parts shown in Figure 2.7b. In general, a simple exact solution for the displacements of each part is possible only when no tensioning stresses are present. When tensioning stresses are present, the displacements can be found using an approximate method such as Rayleigh-Ritz [25]. The accuracy of this method depends on the ability of the assumed shape function to model the exact displacement and, in general, the magnitude of the deflection is slightly underestimated. Here, the exact displacement is not of primary interest, but rather the nature of the solution. Therefore, the simplest admissible displacement functions

$$W_{sym}(x,y) = A_d \, sin\frac{\pi x}{a} \tag{2.25}$$

and

$$W_{skew}(x,y) = C_d \, y \, sin\frac{\pi x}{a} \tag{2.26}$$

are used for the symmetric and skew-symmetric cases respectively.

Using the Rayleigh-Ritz method, the constants A_d and C_d in Equations (2.25) and (2.26) are found. When the tensioning stresses are given by Equation (2.1), the approximate symmetric and skew-symmetric displacements become respectively

$$W_{sym}(x,y) = \frac{\frac{1}{2}F_t a^3}{\pi^3 D}\frac{2\xi}{\pi} sin\frac{\pi x}{a} \tag{2.27}$$

and

$$W_{skew}(x,y) = \frac{\frac{1}{2}F_t a^3}{\pi^3 D}\left[\frac{\pi}{12\xi^2} + \frac{2(1-\nu)}{\pi} + \frac{b^2 h}{2\pi^3 D}\sum_n \frac{(-1)^n}{n^2} A_n\right]^{-1} y \, sin\frac{\pi x}{a} \tag{2.28}$$

$$n = 1,2,3,\ldots$$

Equation (2.27) shows that the tensioning stresses have no effect on the symmetric displacements. This result occurs because the assumed displacement shape has a constant displacement along the width of the plate. In reality, the actual displacement shape does vary slightly across the width of the plate. Therefore, the tensioning stresses do have a small influence on the displacement. However, this influence is very small and is neglected here. In contrast, Equation (2.28) shows that the tensioning stresses significantly affect the skew-symmetric displacements. The influence of the stresses on the skew-symmetric displacements is given by the summation term in Equation (2.28).

The displacement of the plate in Figure 2.7a can be found by superposing Equations (2.27) and (2.28). The maximum displacement is then given by

$$W\left(\frac{a}{2},\frac{b}{2}\right) = \frac{F_t a^3}{\pi^3 D}\left[\frac{\xi}{\pi} + \frac{1}{\frac{\pi}{3\xi} + \frac{8(1-\nu)\xi}{\pi} + \frac{2a^2h}{\pi^3 D\xi}\sum_n \frac{(-1)^n}{n^2}A_n}\right] \qquad n = 1,2,3,\ldots (2.29)$$

Substituting Equations (2.23) and (2.29) into Equation (2.24), the stiffness becomes

$$K = \frac{\pi^2 D}{a^2}\left[\frac{\xi}{2\pi} + \frac{1}{\frac{2\pi}{3\xi} + \frac{16(1-\nu)\xi}{\pi} + \frac{4a^2h}{\pi^3 D\xi}\sum_n \frac{(-1)^n}{n^2}A_n}\right]^{-1} \qquad n = 1,2,3,\ldots (2.30)$$

Figure 2.8 illustrates the influence of tensioning stresses on the plate stiffness described by Equation (2.30). The dimensions of the plate are given in Table 2.1 and the values of stiffness have been normalized with respect to the value for the stress-free plate, 13300 N/m. The

change in stiffness caused by each of the first four terms of Equation (2.1) is shown for the case when the stresses are the same as in Figure 2.3c.

Figure 2.8 shows that the tensile edge stresses increase the stiffness of the plate. However, the increase becomes less as the value of n increases. In a manner similar to the lateral displacement and torsional frequency, the stiffness is most influenced by the lowest terms in Equation (2.1) which describe the "average" of the actual stress distribution. Additionally, the summation term in Equation (2.30) shows that the value for stiffness depends on the cumulative effect of each of the lower stress terms and not on the size of each term individually.

2.6 Simplified relationships

Figure 1.3 shows that in practice, the light-gap profile is used to indicate changes in the stiffness and frequency of a bandsaw caused by tensioning. In the previous sections, relationships are given which describe how the tensioning stresses influence lateral displacement, frequency and stiffness. In this section, these relationships are simplified in order to directly establish how the stress parameters in Equation 2.1 influence bandsaw lateral displacement, torsional frequency and stiffness. By studying the effect of the stress parameters, an indication of the effectiveness of the light-gap method can be obtained.

The expression for lateral displacement given in Equations (2.5) to (2.10) can be simplified by using a binomial expansion for the magnitude term, b_n. By expanding b_n as

$$b_n \approx \frac{A_n}{4\left[\frac{n\pi}{\beta b}\right]^4} - \frac{A_n}{16\left[\frac{n\pi}{\beta b}\right]^8} + \cdots \tag{2.31}$$

and retaining only the first term, Equation (2.5) becomes approximately

$$w(y) \approx w_o(y) - \frac{R}{E}\sum_n \left[\frac{\beta^4 b^4}{4\pi^4}\frac{A_n}{n^4} cos\frac{2n\pi y}{b} + (-1)^n \frac{\beta^4 b^2 R}{\pi^2 \nu}\frac{A_n}{n^2} w_o(y) \right] \qquad (2.32)$$

$$n = 1,2,3,...$$

where the first component, $w_o(y)$, describes the displacement of the stress-free plate and the second component is the approximate change in displacement caused by the tensioning stresses in Equation (2.1).

Equation (2.32) shows that the first term of the change in displacement component is proportional to $A_n n^{-4}$ where A_n is the size of the nth term in Equation (2.1). The second term in the change of displacement component is proportional to $A_n n^{-2}$. Therefore, as n increases, the first term decrease much faster than the second. For values of n larger than about two, the first term becomes small compared to the second and the change in displacement becomes essentially proportional to $A_n n^{-2}$. This relation shows why the size of the $w_n(y)$ curves in Figure 2.3b decreases with increasing values of n.

Equation (2.21) can be simplified to show the influence of the stress parameter, n, and size, A_n, on the torsional frequency of a bandsaw. By expanding the frequency parameter in Equation (2.22) using a binomial expansion and retaining the first two terms, the frequency is approximately given by

$$\omega_{tor} \approx \frac{1}{a^2}\left[\sqrt{\pi^4 + 24\pi^2(1-\nu)\xi^2} + \frac{36(1-\nu^2)\left(\frac{a}{h}\right)^2}{\sqrt{\pi^4 + 24\pi^2(1-\nu)\xi^2}} \sum_n \frac{(-1)^n}{n^2}\frac{A_n}{E} \right]\sqrt{\frac{D}{\rho h}} \qquad (2.33)$$

$$n = 1,2,3,...$$

The first term in Equation (2.33) represents the torsional frequency of the stress-free plate and the second term is the approximate change in frequency caused by the tensioning stresses. The second term shows that the change in frequency is approximately proportional to $A_n n^{-2}$ which is the same approximate relationship obtained for the lateral displacement.

To establish a relationship between the stress parameter, n, and the cutting stiffness, Equation (2.30) can be rewritten as

$$K \approx \frac{\pi^2 D}{a^2}\left[\frac{\pi^3 + 24\pi(1-\nu)\xi^2}{2\pi^2\xi + 12(1-\nu)\xi^2} + \frac{9\pi a^2 h \sum_n \frac{(-1)^n}{n^2} A_n}{4D\xi\left(\pi^2\xi + 6(1-\nu)\xi^2\right)^2}\right] \qquad (2.34)$$

$$n = 1,2,3,\ldots$$

The details of this calculation are given in reference [26].

The first term in Equation (2.34) is the stiffness of the stress-free plate. The second term is the approximate change in stiffness caused by tensioning stresses given by Equation (2.1), and is proportional to $A_n n^{-2}$. This is the same relationship obtained for the lateral displacement and first torsional frequency.

The approximate relationships given above show that the lateral displacement, frequency and stiffness of a bandsaw all consist two components. The first component describes the behaviour of the stress-free plate and the second component describes the changes caused by the tensioning stresses. In each case, the changes caused by the stresses are approximately proportional to $A_n n^{-2}$. These relationships indicate that the same stress components with the

lowest n values most significantly influence the lateral displacement profile, the first torsional frequency and the stiffness. Since all three features respond to tensioning stresses in similar ays, a change in the lateral displacement profile (measured by the light-gap) will be a good indicator of changes in the frequency and stiffness. This theme is explored more fully in subsequent chapters.

3.0 INFLUENCE OF ROLL TENSIONING ON LATERAL DISPLACEMENT, FREQUENCY AND STIFFNESS

3.1 Chapter overview

This chapter describes how roll tensioning influences the lateral displacement, frequency and stiffness of a bandsaw. Although saws are also commonly tensioned by hammering, roll tensioning is the preferred method because it provides faster, more uniform results. In practice, the location of each roller path is known to affect the tensioning state of the saw. The influence of roll path position on lateral displacement, torsional frequency and stiffness is examined in this chapter.

3.2 Influence of roll path position

Figure 3.1 schematically shows a stress distribution resulting from roll tensioning a bandsaw blade. The stresses resulting from several single pairs of roll paths symmetrically placed with respect to the plate centreline are shown for half of the plate. The location of each roll path is indicated by the compressive stress regions which, for simplicity, are modeled as step functions. Each roll path pair is located at a different distance from the plate centreline but has the same magnitude of stress. The roll paths shown in the figure can be used to study the influence of roll path position on the lateral displacement, torsional frequency and stiffness of a bandsaw having dimensions given in Table 2.1. For convenience, each roll path pair is identified by a number from 1 to 5.

Figure 3.2 shows the influence of roll path position on the lateral displacement of a bandsaw

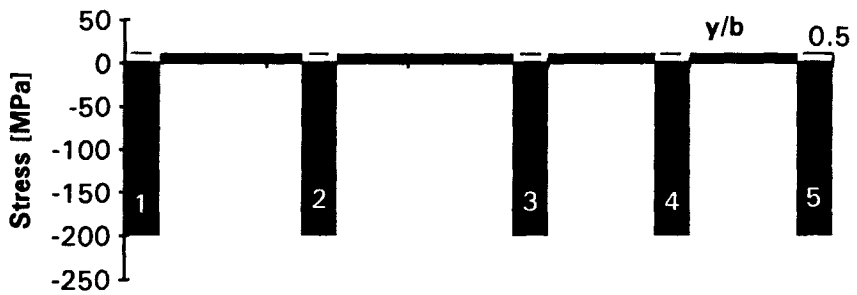

Figure 3.1 Stress distribution for five single roll paths pairs.

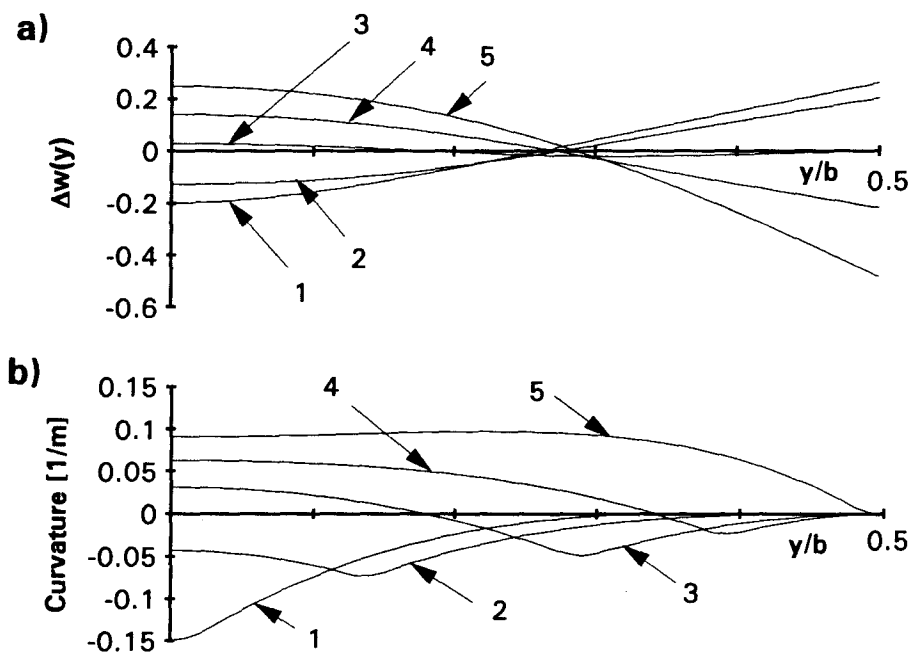

Figure 3.2 Influence of roll path position on a) lateral displacement and b) lateral displacement curvatures.

having dimensions given in Table 2.1. Part (a) of the figure shows the change in displacement, $\Delta w(y)$, associated with each individual roll path pair shown in Figure 3.1. Each displacement curve is labelled with the number of the roll path which is associated with that curve. Again, only half of the displacement profiles need to be shown because of symmetry. The change in displacement curves are calculated from Equation (2.6) after the stress series coefficients, A_n, in Equation (2.1) have been calculated for the associated roll paths using Equation (2.2). The $\Delta w(y)$ curves labelled "1" and "2" are associated with the two innermost roll path pairs and are concave shaped while the curves labelled "4" and "5" are associated with the two outermost roll paths and are convex shaped. The magnitude of the displacements is largest for roll paths at the centre and edges of the plate and decreases as the roll path location approaches a "neutral zone" located at approximately $y/b = 0.3$. In the area near the neutral zone, the $\Delta w(y)$ curves change from the concave shapes of curves 1 and 2 to the convex shape of curves 4 and 5. The curve labelled "3" is associated with the roll path in Figure 3.1 located within the neutral zone. This curve is very small in size and has a convex shape in the central area of the saw and a concave shape near the plate edges.

Figure 3.2b shows the curvatures of the displacement curves in Part (a) of the figure. Negative values of curvature indicate a concave shaped $\Delta w(y)$ curve while positive values indicate a convex shape. Each $\Delta w(y)$ curve has its most concave curvature at the location of the roll path associated with that curve. This occurs because the large compressive stresses in the roll path tend to push the saw blade out of plane when the plate is bent along its length. The curvatures in the remainder of the plate are smaller because the tensile stresses in these areas are relatively small and tend to pull the plate back into plane. The increased concave curvature at the roll path position is important in practice. It allows the shape of a bandsaw's light-gap profile can be adjusted by placing roll paths at various locations along the width of the saw blade. This effect is explored further in subsequent chapters.

Roll path position also influences the frequency and stiffness of a bandsaw. Figure 3.3 shows frequency and stiffness ratios for a tensioned bandsaw having dimensions given in Table 2.1. The saw is tensioned by single pairs of roll paths symmetrically placed on each side of the plate centreline as shown in Figure 3.1. The values of frequency and stiffness are calculated from Equations (2.21), (2.22) and (2.30) for different locations of the individual roll paths. These values are then normalized with respect to the frequency and stiffness of the stress-free plate. Figure 3.3 shows that both the frequency and stiffness increase when the roll paths are in the central region of the plate and decrease when the roll paths are near the plate edges. The change in frequency and stiffness is greatest for roll paths at the centre or edges of the plate and decrease as the roll path position approaches a neutral zone, again located at approximately $y/b = 0.3$.

The analogous behaviors illustrated in Figures 3.2a and 3.3 clearly show the similar ways in which tensioning stresses influence bandsaw lateral displacement, frequency and stiffness. Rolling tensioning in the central region of the saw causes concave shaped displacements and increases frequency and stiffness. Rolling outside of the neutral zone causes convex shaped displacements and decreases frequency and stiffness. Thus, the size and shape of the lateral displacement profile indicates the amount of change in frequency and stiffness. This feature supports the hypothesis illustrated in Figure 1.3 that the light-gap profile is a useful indicator of saw blade frequency and cutting edge stiffness.

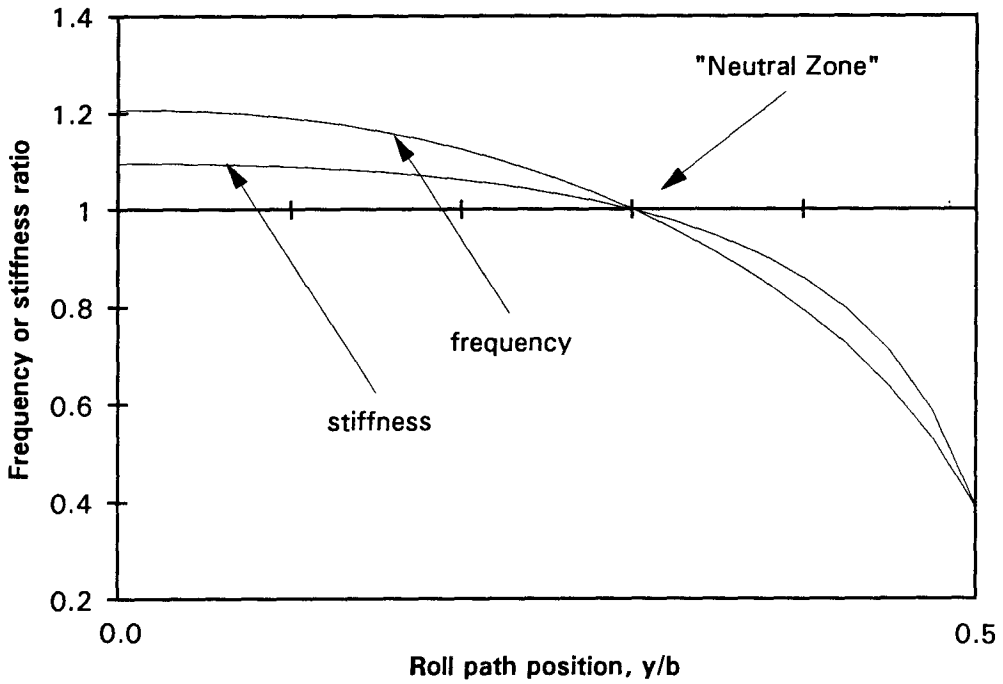

Figure 3.3 Influence of roll path position on frequency and stiffness.

4.0 THE LIGHT-GAP METHOD FOR BANDSAWS

4.1 Chapter overview

This chapter describes how the light-gap method can be used to guide the saw tensioning process. The general procedure for the light-gap method for bandsaws is described in some detail. The traditional light-gap profile is illustrated and significant examples of deviations from this profile are described.

Rules-of-thumb for achieving the desired light-gap profile are given. These rules are explained and are illustrated using an example case of bandsaw tensioning.

4.2 The light-gap method as a guide for the saw tensioning process

Light-gap measurements provide an important guide for the saw tensioning process. The general procedure for the light-gap method involves adjusting the tensioning stresses in a saw so that a specific light-gap profile is achieved. In practice, bandsaws are usually tensioned so that the saw's lateral displacement profile matches the circular shape of a tension gauge in the central region of the saw. The edges of the plate are allowed to fall away from the tension gauge profile and the point where the saw profile leaves the tension gauge curve is called the "tire line". Figure 4.1a shows a tension gauge resting on the surface of a displaced cross section of a saw and illustrates a traditional light-gap profile for a bandsaw.

Localized areas of the saw which do not match the desired light-gap profile are called "tight spots" if they rise toward the tension gauge or "loose spots" if they fall away from the gauge.

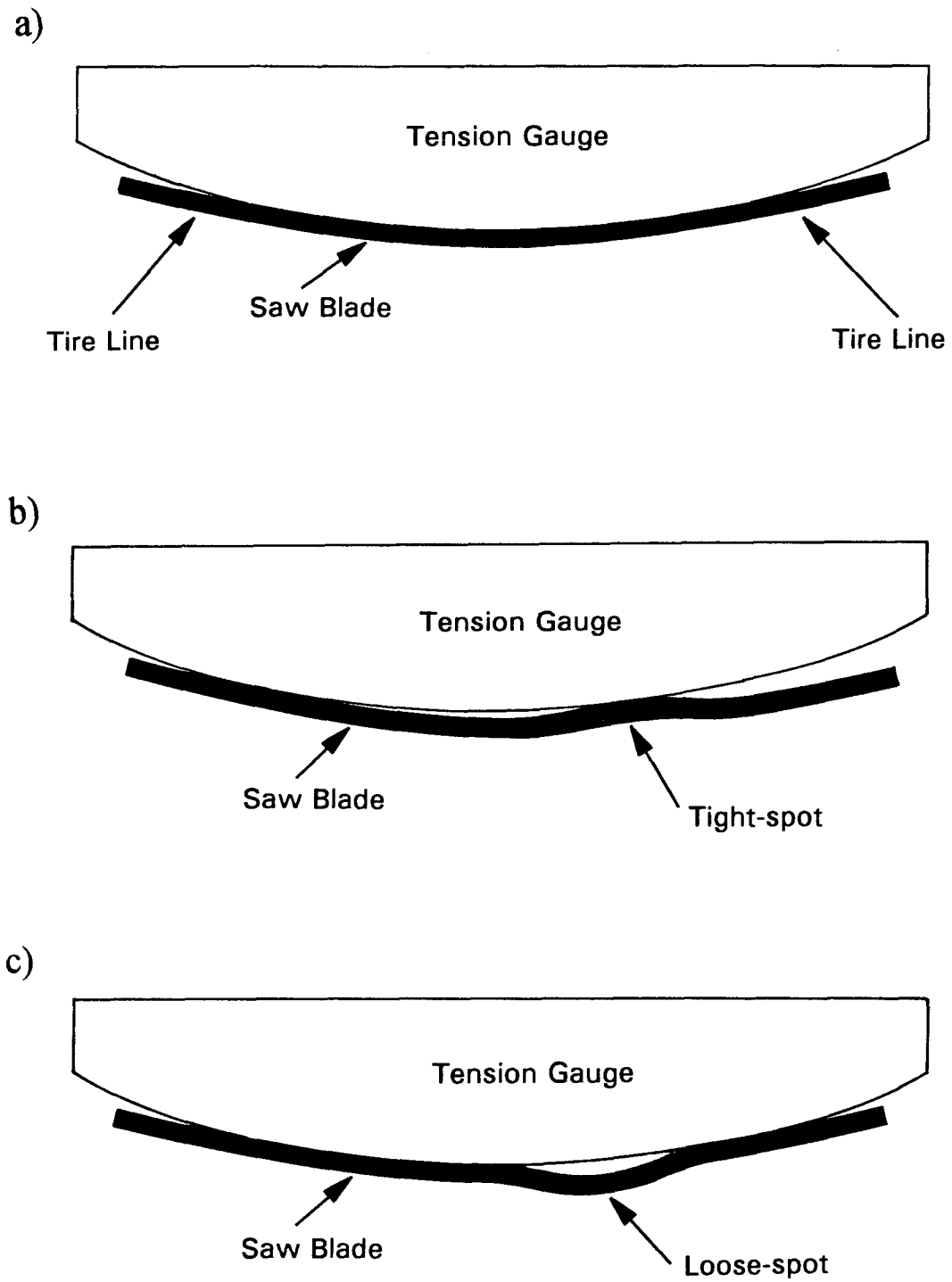

Figure 4.1 Exaggerated light-gap profiles for a bandsaw.
a) Traditional light-gap profile.
b) Tight-spot.
c) Loose spot.

These features are illustrated in Figures 4.1b and 4.1c respectively. In practice, tight and loose spots are considered to indicate local defects in the tensioning state of the saw. These defects are corrected by additional tensioning. By adjusting the position of the additional tensioning rolls, the shape of the light-gap profile can be controlled.

4.3 Rules-of-thumb for obtaining the desired light-gap profile

In order to achieve the traditional bandsaw light-gap profile shown in Figure 4.1a, rules-of-thumb have been empirically developed by sawfilers to enhance the utility of the light-gap method. These rules-of-thumb are used to interpret the information contained in the light-gap profile and to guide the location of roll paths induced during the tensioning process.

The general procedure for tensioning an initially stress-free bandsaw involves placing a number of roll paths in the central region of the saw blade until the light-gap profile assumes the approximate concave shape of the tension gauge. The details of the light-gap are then adjusted by additional rolling to remove any tight or loose spots which may be indicated by the light-gap profile.

The exact locations of the initial roll paths are not important because these rolls are induced only to obtain the basic concave shape of the desired light-gap profile. However, Figure 3.2 indicates that these initial rolls must be placed in the central region of the plate, between the neutral zones at each edge of the plate. Rolls placed in this region have the desired effect of encouraging a concave shaped light-gap. A number of roll paths are usually required to achieve the desired effect.

Once the basic concave light-gap profile is achieved, any tight or loose spots indicated by the

light-gap profile are removed by additional rolling. Tight spots, for example, are localized areas where the curvature of the saw's lateral displacement profile is less than the curvature of the tension gauge. Such tight spots are corrected by rolling the saw plate at the location of the tight spot. Figure 3.2b shows that rolling on the tight spot is effective because the maximum curvature increase is produced at the roll path location. This localized increase in curvature lowers the tight spot relative to the adjacent areas of the saw and enables the lateral displacement profile to match the tension gauge shape.

Loose spots, on the other hand, are areas where the curvature of the lateral displacement profile is greater than the curvature of the tension gauge. By rolling beside the loose spot, the curvature at the loose spot is decreased relative to the curvatures in the rest of the saw. If the loose area has adjacent tight spots, removing the tight spots will often remove or reduce the loose spot. If the loose spot extends across the width of the plate the existing tensioning is excessive. Rolling near the plate edges will decrease the curvature in the central region of the saw and will restore the desired level of tensioning.

Figure 4.2 illustrates an example of the tensioning process described above. The tensioning state for a bandsaw having dimensions given in Table 2.1 is shown at three stages of the tensioning process. At each stage, the stresses, lateral displacement, frequency and stiffness are shown. The compressive regions of the stress distributions indicate the location of each roll path. The roll paths are placed symmetrically on each side of the plate centreline because no backcrown is desired in this case. Only half of the plate are shown in the figure because the lateral displacement profile and the rolling are symmetric about the centreline.

Figure 4.2a shows the state of the saw blade before roll tensioning. The stress-free saw has a convex shaped lateral displacement profile and a first torsional frequency of 53.2 Hz and a stiffness of 13350 N/m.

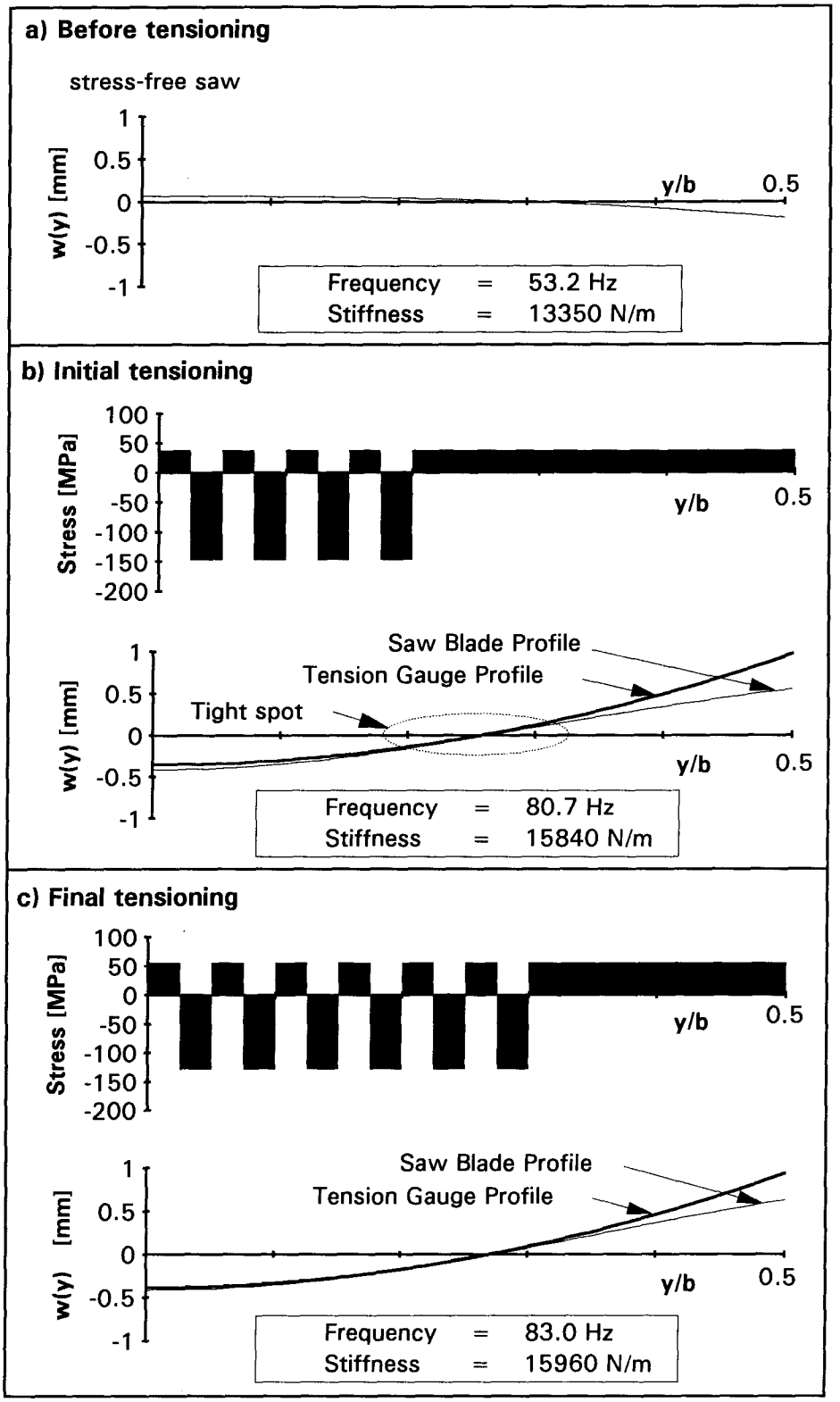

Figure 4.2 Tensioning state at three stages of the tensioning process.

Figure 4.2b shows the tensioning state after the initial roll paths have been placed in the central region of the saw. The first roll paths are placed near the plate centre because rolling at this position results in the greatest change in the lateral displacement. Each additional roll is placed slightly outside the last so that no two roll paths overlap. The four pairs of roll paths shown in the figure result in a lateral displacement profile which is concave in shape and roughly matches the profile of the tension gauge. The tension gauge touches the saw surface in the area around y/b = 0.25. This area is identified as a tight spot.

To obtain the desired light-gap profile, the tight spot in the light-gap profile in Figure 4.2b must be removed. Following the rules-of-thumb for correcting tight spots, two additional roll path pairs are placed at about y/b = 0.25. The resulting tensioning state is shown in Figure 4.2c. The tight spot is relieved and the desired light-gap profile is achieved.

Figure 4.2 shows that tensioning a bandsaw to the traditional light-gap profile increases the frequency and stiffness of the saw. The initial tensioning results in the largest increase in frequency and stiffness while the final adjustments to the light-gap profile typically result in only a small change in these values. For example, the initial tensioning shown in Figure 4.2b results in an increase in frequency and stiffness of 52% and 18% respectively over the values for the stress-free plate in Part (a). However, the final adjustments to the light-gap profile only increase the frequency by an additional 4% and stiffness by an additional 1%.

Although the tensioning example in Figure 4.2 is fairly simple, practical corrections of tight and loose spots is usually an iterative process requiring several cycles of observing the light-gap profile and corrective rolling. The difficulty of obtaining the desired light-gap is further complicated by non-uniformities in the flatness of the saw plate. These "levelling" defects must also be corrected during the tensioning process.

The rules-of-thumb used with the light-gap method are effective in practice because they guide the placement of the roll paths so that the traditional light-gap profile may be readily achieved. This is a significant advantage over the frequency method of saw tensioning evaluation, which does not provide any guidance to corrective actions. Furthermore, by tensioning a bandsaw to the traditional light-gap profile, the torsional frequency and stiffness of the saw are increased and cutting performance is enhanced.

5.0 ADDITIONAL FACTORS INFLUENCING LIGHT-GAP MEASUREMENTS

5.1 Chapter overview

This chapter discusses some of the additional factors which influence light-gap measurements. The effect of the curvature applied along the length of a bandsaw blade on the light-gap profile is discussed, as well as the significance of the size of the "tire-lines" in the traditional light-gap profile.

5.1 Influence of applied curvature on the light-gap profile.

The light-gap profile for a bandsaw blade is produced by bending an initially flat saw blade along its length. The applied curvature, R, shown in Figure 2.2 causes a corresponding lateral deflection across the width of the saw. Equations (2.6) to (2.10) show that the value of R influences the size and shape of the light-gap profile of a bandsaw. Foschi investigated this effect for the special case of a rectangular plate containing parabolically distributed tensioning stresses [21]. However, in general, tensioning stresses are more easily approximated using the Fourier cosine series in Equation (2.1). This section investigates the influence of the applied curvature, R, on the size and shape of the light-gap profile when the tensioning stresses are given by Equation (2.1).

The size of the light-gap profile, δ can be defined as

$$\delta = w(0) - w(b/2) \tag{5.1}$$

where w(0) and w(b/2) are the values of lateral deflection given by Equation (2.5) at the centre and edge of the plate respectively. When the tensioning stresses are given by Equation (2.1), Equation (5.1) can be rewritten in non-dimensional form as

$$\frac{\delta}{h} = C\nu\varepsilon - \sum_n \frac{\alpha_n}{C + C\left[\frac{n\pi}{\gamma\sqrt{C}}\right]^4}\left[\left(1-(-1)^n\right) + 4n^2\pi^2(-1)^n\varepsilon\right] \qquad n = 1,2,3,\ldots \tag{5.2}$$

where

$$C = \frac{b^2}{Rh} \tag{5.3}$$

$$\alpha_n = \frac{A_n}{E}\left[\frac{b}{h}\right]^2 \tag{5.4}$$

$$\gamma = \sqrt[4]{3(1-\nu^2)} \tag{5.5}$$

$$\varepsilon = A^*\left(1 - \cosh\frac{\gamma\sqrt{C}}{2}\cos\frac{\gamma\sqrt{C}}{2}\right) - B^*\sinh\frac{\gamma\sqrt{C}}{2}\sin\frac{\gamma\sqrt{C}}{2} \tag{5.6}$$

and

$$A^*, B^* = \frac{\sinh\frac{\gamma\sqrt{C}}{2}\cos\frac{\gamma\sqrt{C}}{2} \mp \cosh\frac{\gamma\sqrt{C}}{2}\sin\frac{\gamma\sqrt{C}}{2}}{\gamma^2 C\left(\sinh\gamma\sqrt{C} + \sin\gamma\sqrt{C}\right)} \tag{5.7}$$

δ/h in Equation (5.2) is the size of the light-gap profile relative to the plate thickness, h, while the parameter, C, provides a non-dimensionalized measure of the applied curvature, R.

Figure 5.1 shows the relationship between the size of the light-gap profile, δ/h, and the applied

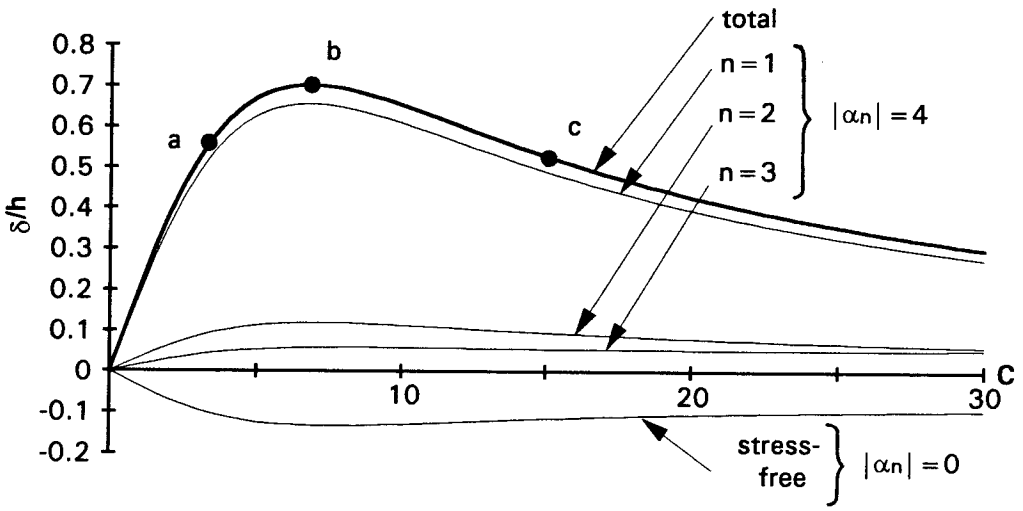

Figure 5.1 Influence of applied curvature on light-gap size.

curvature parameter, C. Several curves are shown in the figure. The first curve, labelled "stress-free", shows the size of the light-gap profile for an untensioned saw. This curve is described by just the first term in Equation (5.2) because the stress parameters, α_n, are all identically zero. The light-gap size for the stress-free plate is negative because the displaced shape of the saw is anticlastic.

The curves labelled "n=1", "n=2" and "n=3" in Figure 5.1 show the influence of the first three components of tensioning stress on the size of the light-gap profile. These curves are described by the second term in Equation (5.2) for the case when the stress parameter, α_n, has a magnitude of ± 4. The curve labelled "n=1" shows the effect of just the first component of stress, while the curves labelled "n=2" and "n=3" show the individual effects of the second and third components of stress. Each of these curves are positive because the sign of the stress parameter is chosen so that the resulting displacement component is concave in shape.

The curve in Figure 5.1 labelled "total" is the sum of the other curves in the figure. This curve shows the influence of the applied curvature on the size of the light-gap profile for the special case of a rectangular plate containing the tensioning stress components indicated in the figure.

Figure 5.1 shows that when the bandsaw blade is initially flat, that is C=0, the light-gap size is also zero. As the applied curvature is increased, the size of δ/h rapidly increases to a maximum value before decreasing at higher values of C. The value of C which results in the maximum light-gap, C^*, depends somewhat on the tensioning stresses in the saw. This is because each curve describing the effect of the nth component of stress has a maximum at a slightly different value of C. For example, the n=1 curve in Figure 5.1 has a maximum at about C=7 while the n=3 curve has a maximum at about C=8.5. Therefore, the applied curvature which results in the maximum light-gap size depends on the size of the first few stress terms in Equation (2.1) which describe the tensioning stresses. In the example given in

Figure 5.1, the maximum light-gap indicated by the "total" curve occurs at about $C^*=7$.

Figure 5.2 shows the influence of the applied curvature, R, on the shape of the light-gap profile. Part (a) shows half of the lateral displacement profile for a bandsaw having dimensions given in Table 2.1 and containing the same tensioning stresses as the example in Figure 5.1. The curves labelled "a", "b" and "c" show the lateral displacement profile at corresponding points on the δ/h curve in Figure 5.1. Curve b in Figure 5.2 shows the lateral displacement profile when the value of the curvature parameter, C^*, corresponds to the largest light-gap size. Curves a and c show the lateral displacement profile when the curvature parameter is, respectively, less than and greater than C^*.

Figure 5.2 shows that the applied curvature influences the shape as well as the size of the light-gap profile. This effect can be more easily seen from the curvatures of the lateral displacement profiles which are shown in Part (b) of the figure. The curvatures of curves a and b have different values because they have different light-gap sizes. However, the shape of the curvature profiles is almost the same indicating that the two lateral displacement profiles in Figure 5.2a have essentially the same shape. This implies that for values of C less than C^*, the shape of the light-gap profile is relatively constant. For values of C greater than C^*, the shape of the light-gap profile changes. The curvature of curve c is much different than for curves a or b. Curve c is less concave in the central region of the saw and is more convex near the plate edges. This indicates that the central region of the saw becomes flatter and the plate edges become more curved when the curvature parameter increases beyond C^*.

Because the applied curvature influences both the size and shape of the light-gap profile, the size of the applied curvature must be controlled to achieve repeatable results. The empirical choice of a tension gauge curvature implicitly takes into account the value of C used. Thus, once the tension gauge curvature and the value of the applied curvature have been established,

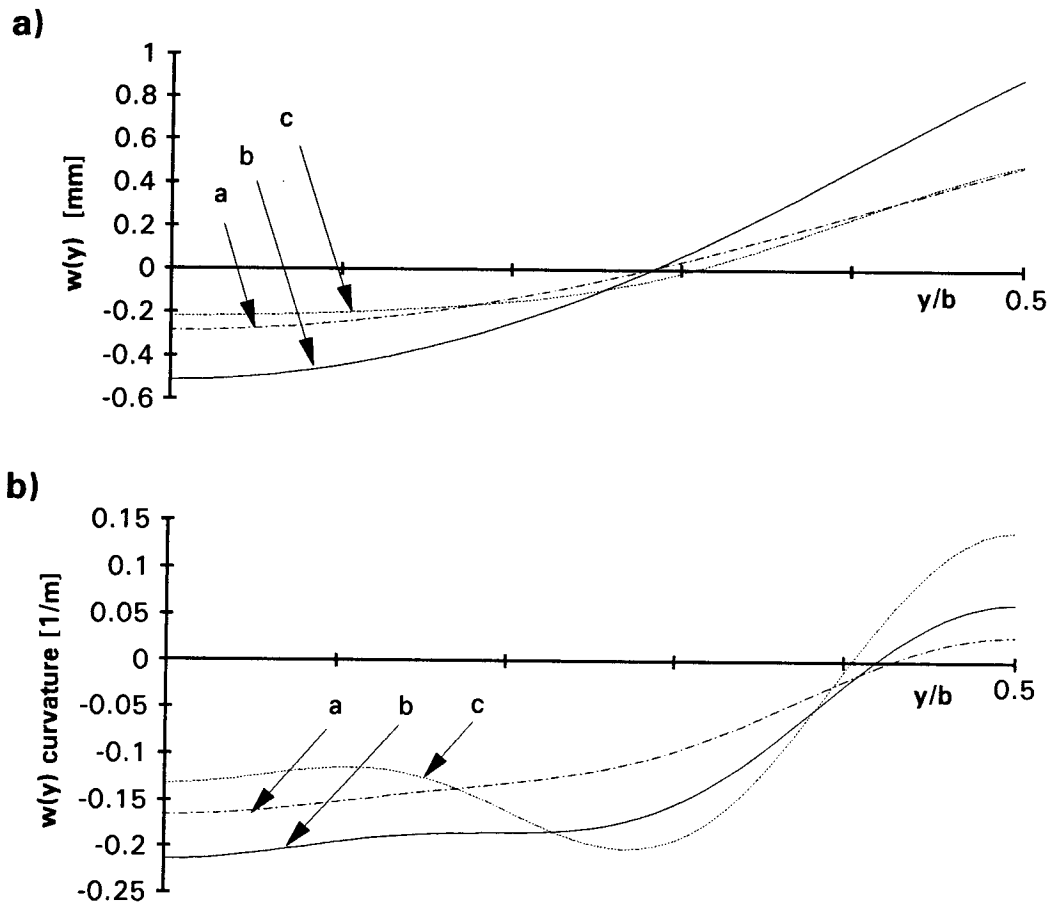

Figure 5.2 Influence of the applied curvature on the light-gap profile.
a) Lateral displacement profiles.
b) Curvatures of the displacement profiles in a).

consistency becomes the issue.

In practice, the size of the applied curvature can be controlled in several ways. One method involves adjusting the curvature so that the maximum light-gap size is obtained. Another method involves supporting the saw blade between two fixed points and allowing the saw to sag under its own weight. Either of these methods can produce good results. As long as the same method is consistently used, the exact value of the applied curvature is not of practical concern.

5.3 Significance of tire size

In the traditional light-gap profile shown in Figure 4.1a, the edges of the tensioned bandsaw fall away from the tension gauge profile. The point where the plate falls away from the tension gauge is called the "tire line" and the region outside this point is called the "tire". In practice, there is often considerable variation in the size of the tire used by different sawfilers. The significance of these variations in tire size is not well understood. This section investigates the influence of tire size on bandsaw frequency, stiffness and tensioning stress.

Figure 5.3 shows two different tensioning states for a bandsaw having dimensions given in Table 2.1. The tensioning stresses, light-gap profile and frequency and stiffness are given for each case. Each of the tensioning stresses have been adjusted so that the resulting lateral displacement profiles match the same sized tension gauge, but have a different sized tire.

The stress distribution shown in Figure 5.3a results from roll paths placed in the central two thirds of the saw plate, between the neutral zones near each edge of the plate. Roll paths placed in this region increase both the frequency and stiffness of the saw. The resulting light-

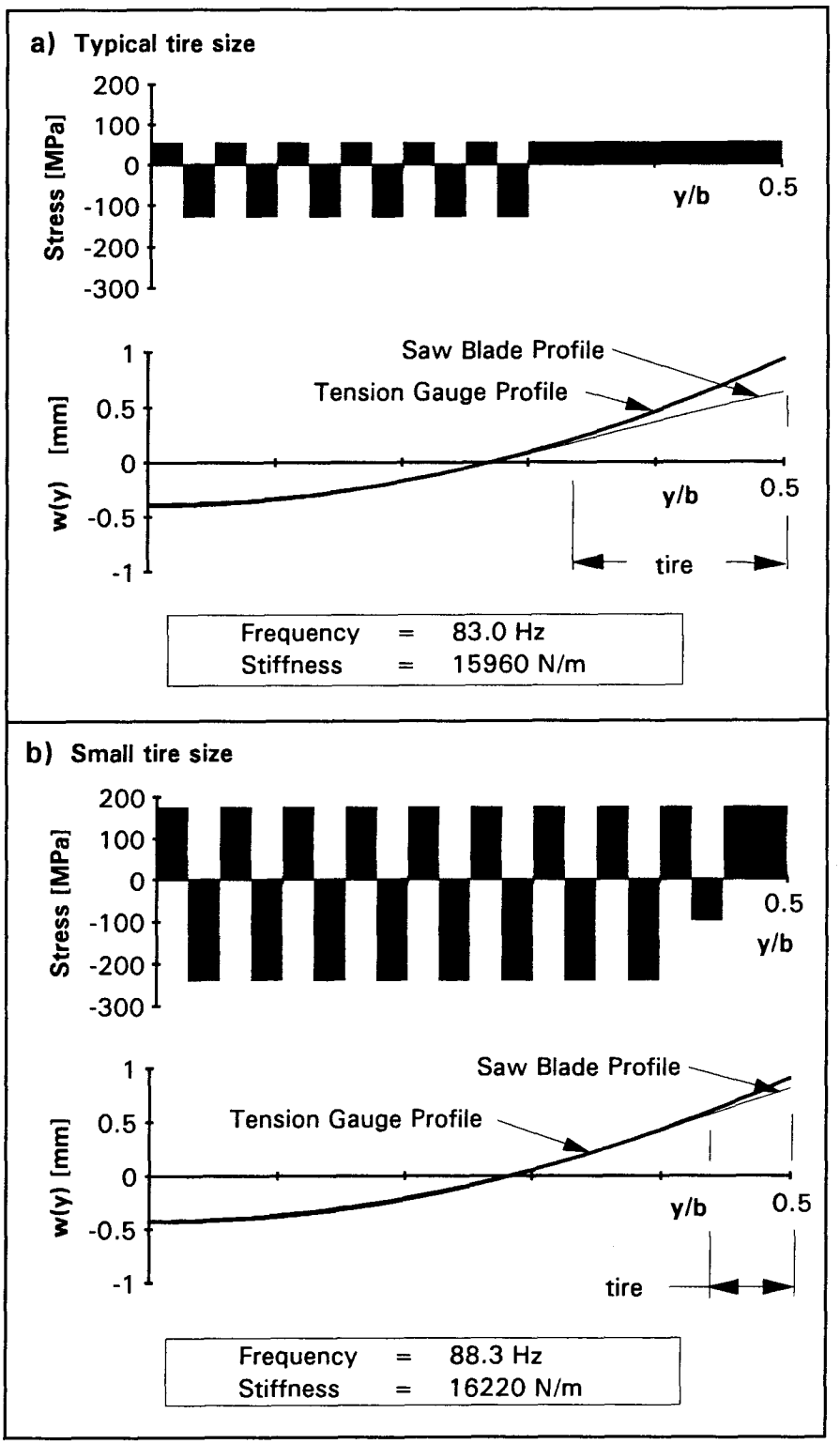

Figure 5.3 Influence of tire size on frequency, stiffness and stresses.

gap profile matches the tension gauge shape in the central region of the saw and has a tire area extending from y/b = 0.33. The frequency and stiffness of the saw plate are 83.0 Hz and 15960 N/m respectively.

The stresses shown in Figure 5.3b have been adjusted so that the resulting lateral displacement profile matches the same size tension gauge shown in Part (a) of the figure but has a smaller tire. In this case the tire extends from y/b = 0.44, the frequency is 88.3 Hz and the stiffness is 16220 N/m. These values of frequency and stiffness are about 6 percent and 1 percent, higher, respectively, than the values for the plate in Part (a).

The stress distribution in Figure 5.3b associated with the small tire size has roll paths placed outside of the neutral zones of the saw. Because rolling outside the neutral zone reduces tensioning, excessively large roll paths are required in the central region of the saw to counteract the loss of tensioning. The large compressive stresses induced by heavy rolling result in correspondingly large tensile stresses in the remainder of the plate. For example, the plate in Figure 5.3b has tensile stresses of 176 MPa which is more than three times higher than the plate in Part (a) which has tensile stresses of 55.3 MPa.

In general, achieving a small tire size by roll tensioning outside of the neutral zone results in a slight increase in the frequency and stiffness of a bandsaw but also results in large tensile tensioning stresses. In practice, large tensile stresses at the plate edges are undesirable in bandsaws. Bandsaws are subject to fatigue related cracking at the saw tooth gullets caused by a combination of stress concentrations from the tooth grinding, the tooth profiles and large tensile stresses at the plate edges. The tensile stresses during saw operation are caused by a combination of cyclical bending stresses which occur as the saw blade passes over the bandmill wheels and uniform tensile stress caused by bandmill strain. Large tensioning stresses further increase the tensile stresses at the plate edges and can significantly reduce the

fatigue life of a bandsaw. Therefore, in order to control the size of the tensile stresses in a bandsaw, tire size should be wide enough so that roll tensioning in the area outside the neutral zones can be avoided. This can be done by specifying that the tire lines should be approximately at the neutral zones. An approximate rule-of-thumb is, therefore, that the saw should fit the tension gauge profile over the middle two thirds of the blade.

6.0 THE EFFECTIVENESS OF THE LIGHT-GAP METHOD FOR BANDSAWS

6.1 Chapter overview

The light-gap profile can be used to indicate changes in saw plate frequency and stiffness caused by the tensioning stresses. Section 2.6 showed that the components of stress that most influence the frequency and stiffness of a bandsaw similarly influence the size of the light-gap. However, the shape of the light-gap profile is also an important indicator of the tensioning state. In this chapter, the relationships between the shape of the light-gap profile and the frequency and stiffness of a bandsaw are investigated. The effectiveness of the light-gap method for indicating changes in the frequency and stiffness of a tensioned saw is also discussed.

6.2 Relationships between light-gap profile, frequency and stiffness

In this section, the relationships between the light-gap profile, frequency and stiffness are investigated for two cases. The first case involves a bandsaw tensioned to a specific frequency and stiffness while the second case involves the same saw tensioned to a specific light-gap profile.

Figure 6.1 shows three possible tensioning states for a rectangular plate having the dimensions given in Table 2.1. In each case, the tensioning stress and resulting lateral displacement profile, w(y), are shown. Each of the stress distributions have been chosen so that the frequency and stiffness of the plate are the same for each case. Each stress distribution provides an example of how a bandsaw blade could be roll tensioned to a specified frequency,

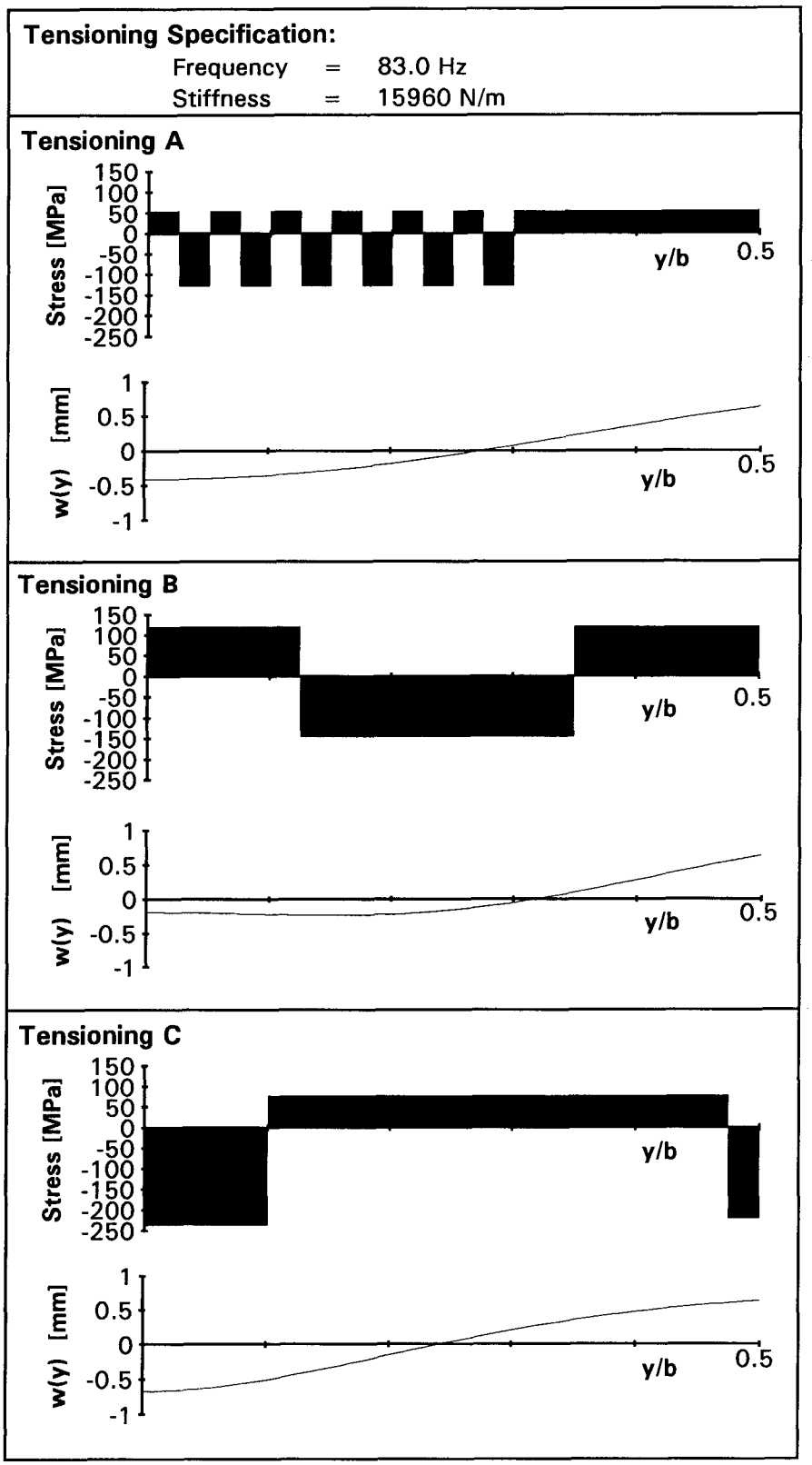

Figure 6.1 Lateral displacement profiles for three different stress distributions producing the same specified values of frequency and stiffness.

rather than the more usual practice of tensioning to a specified light-gap profile.

Tensioning A stresses represent a typical case where the bandsaw has been rolled along several paths in the central region of the plate. Tensioning A is the same as the example shown in Figure 4.2c and provides an example of typical tensioning stresses for a new saw. Tensioning B stresses result from placing adjacent roll paths halfway between the centre and edge of the plate. Tensioning C stresses result from excessive rolling at the plate centre followed by rolling at the plate edge to reduce the frequency and stiffness values to the desired level.

Figure 6.1 shows the lateral displacement profiles for each of the three different tensioning states. The shape of each lateral displacement profile is different, even though the frequency and stiffness is the same in each case. Therefore, tensioning a saw to a specific frequency or stiffness produces light-gap profiles that are not unique.

The non-uniqueness in the lateral displacement profiles in Figure 6.1 is caused by differences in the associated stress distributions. Table 6.1 lists the first five values of A_n for each of the stress distributions in the figure. The columns labelled "frequency" list the natural frequency of the plate subject to the cumulative influence of the stresses corresponding to the coefficients, A_n. The first listed frequency, 53.2 Hz, is for an untensioned saw. The next frequency adds the effect of A_1, the next includes both A_1 and A_2, and so on. Although the three stress fields illustrated in Figure 6.1 have different individual coefficients, Table 6.1 shows that the frequencies of the plates quickly converge to approximately the same value. However, as discussed in Section 2.3, the size and shape of the lateral displacement profile depends on the size of each of the lower A_n coefficients individually. The three tensioning states have different lower values of A_n, and therefore have different "average" stress distributions. These differences in the "average" stress distribution cause the differences in the

Table 6.1 Plate frequencies and stress series coefficients for the tensioning cases in Figure 6.1.

n	Tensioning A		Tensioning B		Tensioning C	
	A_n [MPa]	Freq [Hz]	A_n [MPa]	Freq [Hz]	A_n [MPa]	Freq [Hz]
none	-	53.2	-	53.2	-	53.2
1	-49.7	81.0	-17.4	64.4	-88.3	97.3
2	25.6	83.9	166.7	85.3	-125.1	84.4
3	12.4	83.3	22.7	84.1	-34.9	86.1
4	-10.7	83.0	-25.1	83.4	-57.6	84.5
5	9.7	82.9	10.0	83.3	27.0	84.0
all	-	83.0	-	83.0	-	83.0

Table 6.2 Plate frequencies and stress series coefficients for the tensioning cases in Figure 6.2.

n	Tensioning A		Tensioning D		Tensioning E	
	A_n [MPa]	Freq [Hz]	A_n [MPa]	Freq [Hz]	A_n [MPa]	Freq [Hz]
none	-	53.2	-	53.2	-	53.2
1	-49.7	81.0	-48.0	80.2	-51.0	81.6
2	25.6	83.9	16.9	82.2	15.8	83.4
3	12.4	83.3	-14.2	82.9	10.5	82.9
4	-10.7	83.0	-0.9	82.9	-12.8	82.5
5	9.7	82.9	-38.2	83.6	0.00	82.5
all	-	83.0	-	83.2	-	82.6

lateral displacement profiles. The stiffness of a saw is closely related to its natural frequency and behaves in a similar manner.

Figure 6.2 shows three possible tensioning cases which result when the rectangular plate in Table 2.1 is roll tensioned to the specific light-gap profile shown in the figure. For each case, the size and location of each roll path is chosen so that the lateral displacement of the plate matches the curvature of the tension gauge in the central region. Again, Tensioning A is the same as in Figure 4.2c, while Tensioning D and E are two examples of the many different stress distributions which could also be used to obtain the same specified light-gap profile. The frequency and stiffness values resulting from the three stress distributions are given in the figure and are virtually the same for each case.

In spite of the differences in the details of the stress distributions in Figure 6.2, Table 6.2 shows that the size of the first two stress coefficients are almost the same in each case. Because the shape of the displacement profile depends most strongly on the first two coefficients, the light-gap profiles are also essentially the same. Similarly, the frequency and stiffness also depend most strongly on the lowest terms in the stress series. Table 6.2 shows that the first two stress terms result in a frequency which has already almost converged to the final value. In a similar manner, the stiffness of each plate also rapidly converges.

Figures 6.1 and 6.2 show that although the lateral displacement profile for a given frequency and stiffness is non-unique, the opposite relationship does exist. That is, when a saw is tensioned to a specific light-gap profile, the frequency and stiffness are effectively determined. This behaviour occurs because the frequency and stiffness depend on a weighted sum of the A_n terms. The individual A_n values can be varied as long as the weighted sum remains constant. In contrast, the lateral displacement profile depends on the individual values of A_n. A particular light-gap shape automatically specifies a specific weighted sum and therefore a

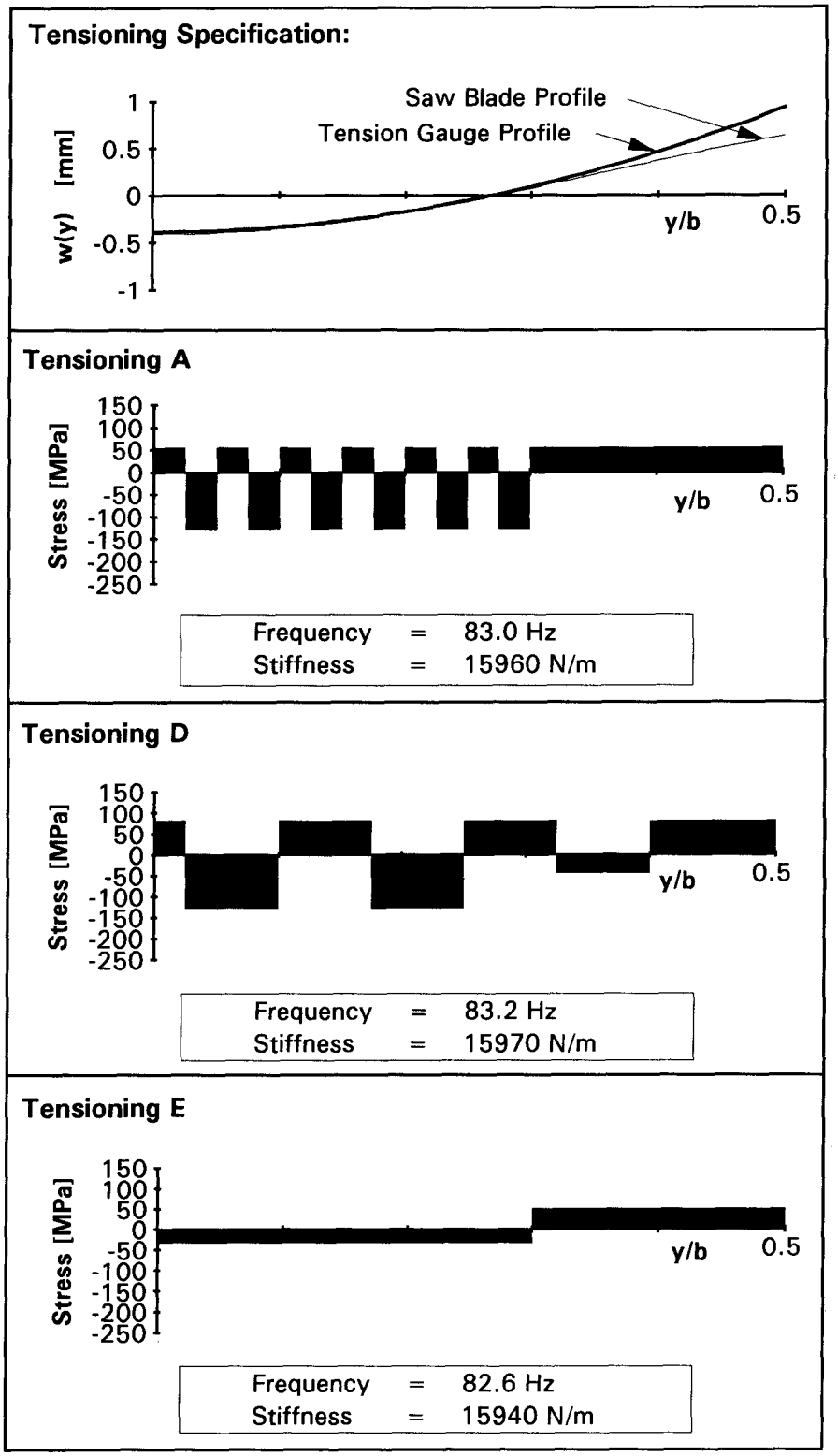

Figure 6.2 Frequency and stiffness values for three different stress distributions producing the same specified light-gap profile.

specific frequency and stiffness. Clearly, the reverse is not true. A particular weighted sum (frequency and stiffness) does not specify the individual A_n values (light-gap).

6.3 The light-gap profile as an indicator of frequency and stiffness

The results of the previous section show that when a saw is tensioned to a specific lateral displacement profile, the frequency and stiffness are effectively determined. This relationship is crucial in practice. It means that the light-gap method does provide an effective way of evaluating the influence of the tensioning stresses on saw performance.

Although a number of different lateral displacement profiles could be used with the light-gap method, the traditional circular profile has a number of practical advantages. Tensioning a saw to this profile requires roll tensioning in the central region of the saw blade which results in a stress distribution with a large n=1 stress term. Figures 2.6 and 2.8 shows that this stress term has the largest influence on frequency and stiffness for a given level of stress. Therefore, tensioning a bandsaw to the traditional light-gap profile results in a large increase in saw frequency and stiffness. Additionally, a circular shaped tension gauge is convenient because it can be used with different widths of bandsaws. Other tension gauge shapes would require special gauges for each bandsaw width.

Most importantly, however, by tensioning a bandsaw to the traditional circular shaped light-gap profile, the curvature of the tension gauge can be used to indicate the frequency and stiffness of the saw. Figure 6.3 illustrates the relationship between tension gauge diameter and saw frequency and stiffness for the specific case of a plate having dimensions given in Table 2.1. The values of frequency and stiffness are normalized with respect to the values for the stress-free plate. Each point on the curve corresponds to a plate tensioned to the traditional

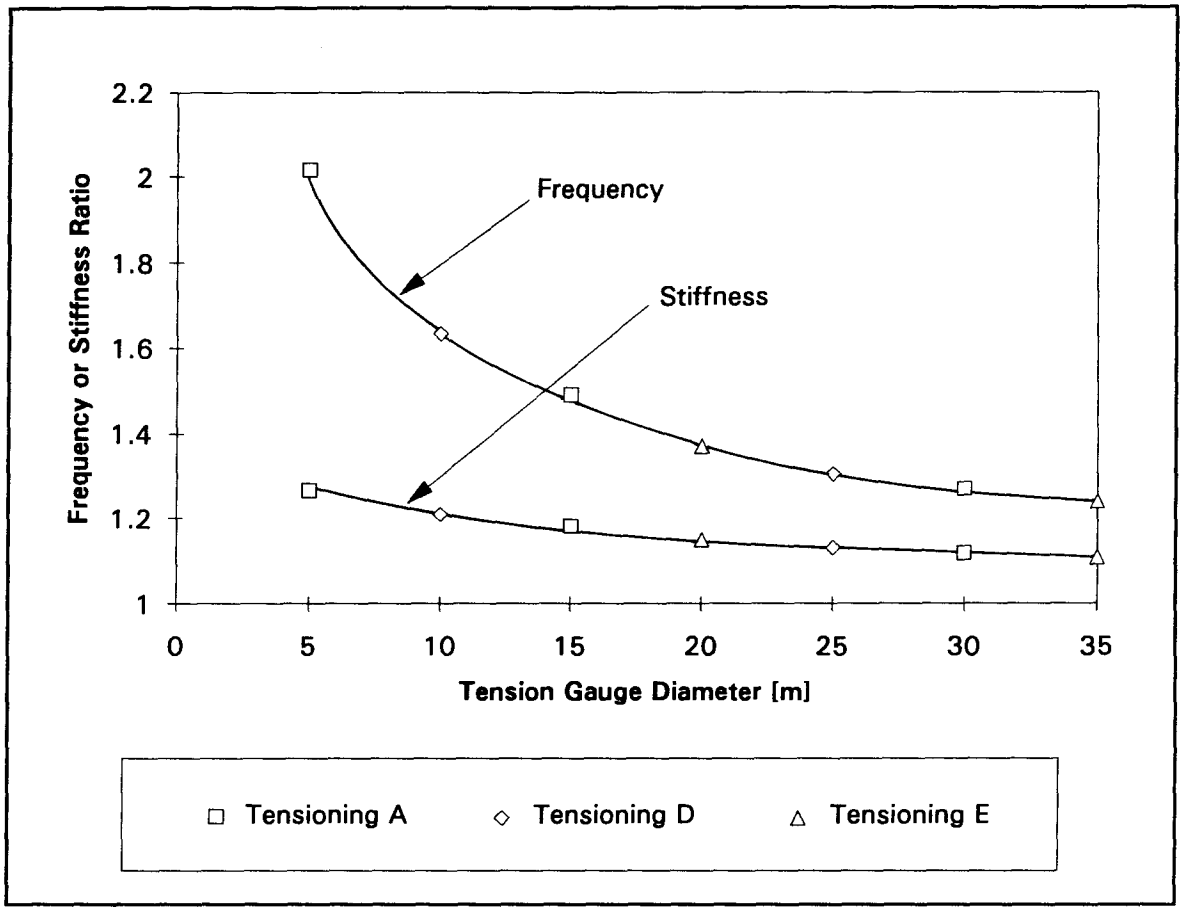

Figure 6.3 Relationship between tension gauge diameter and frequency and stiffness ratio.

light-gap profile and having one of the three stress distributions shown in Figure 6.2. The magnitudes of the stresses have been adjusted so that the resulting lateral displacement matches the various tension gauge diameters.

Figure 6.3 indicates that by specifying the shape of a bandsaw's lateral displacement profile, the size of the profile indicates the frequency and stiffness of the saw. For a saw tensioned to the traditional light-gap profile, as is the case here, the frequency and stiffness of the plate are effectively indicated by the tension gauge diameter. As the tension gauge diameter decreases, the frequency and stiffness of the saw increase. At very small gauge diameters, however, the tensioning stresses may become large enough to buckle the unstrained saw blade, in which case the results in the figure would not be applicable. As the tension gauge diameter becomes very large, the tension gauge shape approaches a straight-edge and the associated frequency and stiffness ratios approach values somewhat greater than unity. This occurs because a stress-free plate has an anticlastic shape and therefore, a small amount of tensioning is required to achieve a flat lateral displacement profile.

The results from Figure 6.2 and 6.3 confirm the hypothesis in Figure 1.3 that the light-gap profile is an effective indicator of saw blade frequency and stiffness. When a saw is tensioned to a specific light-gap profile, the frequency and stiffness are effectively determined. In particular, when a bandsaw is tensioned to the traditional light-gap profile, the frequency and stiffness are indicated by the curvature of the associated tension gauge. Because of these features, the light-gap method provides a rational and effective way of monitoring the saw tensioning process.

7.0 PRACTICAL ADVANTAGES AND LIMITATIONS OF THE LIGHT-GAP METHOD

7.1 Chapter overview

The light-gap method is widely used in industry is because it has a number of important practical advantages over other tensioning evaluation techniques, such as natural frequency measurements. However, the light-gap method also has some limitations. Several of these advantages and limitations are discussed in this chapter.

7.2 Advantages and limitations

One of the most important advantages of the light-gap method is its ability to indicate the tensioning state within a localized part of the saw. The light-gap profile indicated by a tension gauge is influenced by the tensioning stresses in the area near the gauge. Therefore, undesirable variations in the tensioning stresses can easily be identified by moving the tension gauge along the length of the bandsaw. Frequency measurements, on the other hand, provide only a global average of the tensioning state of a saw. Non-uniformities in the tensioning stresses are not indicated.

Another advantage of the light-gap method is its ability to indicate deviations from plate flatness. These "levelling defects" are readily identified by moving a straight-edge over the surface of a saw when it is resting on a flat surface. Because correcting levelling defects influences the tensioning of a saw, levelling and tensioning are usually performed simultaneously. The light-gap method provides a convenient way to monitor the progress of both of these operations. Frequency measurements provide almost no indication of levelling

defects.

One of the limitations of the light-gap method is that the evaluation of the shape of the light-gap profile is somewhat subjective in nature and relies on the skill and judgment of the sawfiler. This can lead to significant variations among saws tensioned by different sawfilers. However, these variations can be reduced by following good industrial practices. For example, saws should be sufficiently flat so that their lateral displacement can be exactly matched to the shape of the tension gauge. Sawfilers often leave the central region of the saw slightly loose so that levelling defects do not interfere with the light-gap profile. This practice limits the accuracy of the light-gap method.

Unlike the light-gap profile, frequency measurements have the advantage of providing a quantitative measure of the tensioning state of a saw and are not affected by small levelling defects. Acceptable ranges for saw frequencies can be specified and used as controls for the saw tensioning state.

In general, the light-gap method is preferred over other tensioning evaluation techniques because it is simple and fast to use, and it provides localized tensioning and levelling information simultaneously. However, the frequency measurement method, by providing a quantitative measure, has the potential to reduce the variability in tensioning among saws.

Ideally, a combination of the light-gap and frequency measurement methods would be extremely effective for controlling the tensioning process. However, because of the difficulty in supporting a bandsaw effectively, frequency measurements are only practical for circular saws. For a circular saw, the light-gap method would be used to tension and level the saw and to ensure that the tensioning state is reasonably uniform. Frequency measurements would then by made as a final check to ensure that the tensioned saw had frequency values falling

within a small specified range. If frequency measurements indicated adjustments to the saw tensioning were required, these adjustment could be easily made by additional roll tensioning. Because the required frequency adjustments would typically be fairly small, the additional roll tensioning would not significantly affect the light-gap profile.

8.0 CONCLUSIONS

The effectiveness of the light-gap method for monitoring the saw tensioning process has been investigated in this thesis. The relationships between tensioning stresses, lateral displacement, first torsional frequency and cutting edge stiffness were studied for the specific case of a bandsaw containing symmetric in-plane tensioning stresses. Although the results presented apply specifically to bandsaws, the general features of the light-gap method are also expected to apply to circular saws.

The light-gap method has been criticized as being a poor indicator of saw tensioning because of its subjective nature and because it is insensitive to the details of the tensioning stress distribution. However the light-gap method is widely accepted in industry, and is used with substantial success to monitor the saw tensioning process. The relationships given in this thesis show that the light-gap method provides an effective measure of bandsaw frequency and stiffness. This occurs because the same components of stress which most influence the torsional frequency and cutting edge stiffness have a similar influence on the light-gap profile.

Both the size and shape of the light-gap profile are important indicators of the tensioning state of a saw. The light-gap profile for a bandsaw depends on the individual size of the lowest few terms in the Fourier series which describes the tensioning stresses. Specifying the size and shape of the light-gap profile controls the size of each of the first few stress terms. This automatically specifies the weighted sum of these terms, on which the plate frequency and stiffness depend. Therefore, by tensioning a bandsaw to a specific light-gap profile, the frequency and stiffness of the saw are indicated.

To achieve effective results with the light-gap method, the shape of the light-gap profile must

be specified. The traditional circular shaped light-gap profile provides a convenient shape. It encourages the tensioning stress components which result in the largest increase in frequency and stiffness for a given stress level. However, the size of the tire areas in the traditional profile must be controlled in order to avoid excessive levels of tensioning stress which can lead to saw cracking problems. Most importantly, however, by using the traditional circular shaped light-gap profile, changes in saw frequency and stiffness are indicated by the size of the curvature of the associated tension gauge. In this manner, the light-gap method provides a reliable and highly effective means of evaluating the affect of the tensioning process on saw performance.

Empirical rules-of-thumb used with the light-gap method guide roll path location in order to achieve the traditional light-gap profile. These rules-of-thumb are effective because roll path position influences the size and shape of the light-gap. Rolling in the central region of the saw plate encourages a traditional concave shaped light-gap profile and increases the torsional frequency and stiffness of a bandsaw. Rolling near the plate edges has the opposite effect. The largest effects are obtained by rolling at the plate centre or edges and decrease as roll path position approaches a "neutral zone". Rolling within the neutral zone has a negligible effect on the light-gap, frequency or stiffness.

In addition to its ability to indicate saw frequency and stiffness, the light-gap method also has a number of practical advantages over other tensioning evaluation techniques such as frequency measurement. The light-gap profile indicates local non-uniformities in the tensioning state, can be used to indicate levelling defects, and is simple and easy to use. In contrast, natural frequency measurements provide only a global average of the tensioning state and so do not indicate local variations. Additionally, frequency measurements do not indicate levelling defects and require sophisticated equipment.

Although the light-gap method has the limitation of providing a somewhat quantitative measure of saw tensioning, this difficulty can be reduced by following good industrial practices. Levelling defects should be reduced as much as possible and the saw should be tensioned to exactly fit the tension gauge shape. The size of the curvature applied along the length of a bandsaw must also be controlled to achieve consistent results with the light-gap method.

Ideally, a combination of light-gap and frequency measurements could improve the quality of saw tensioning. A saw would first be tensioned using the light-gap method and would then be checked using the more quantitative frequency measurements. This procedure has the potential to reduce tensioning variation between saws. However, it would be only practical for circular saws because of the difficulties in making bandsaw frequency measurements.

In summary, the light-gap method provides a reliable and highly effective means of monitoring the saw tensioning process. It can indicate changes in saw frequencies and stiffness caused by the tensioning process and has a number of important practical advantages over other methods.

REFERENCES

1. Statistics Canada. 1989. Wood Industries. Catalog 35-250, Statistics Canada, Ottawa, Ont.

2. Hallock, H. 1962. A mathematical analysis of the effects of kerf width on lumber yield for small logs. Report No. 2254, USDA Forest Service, Forest Products Laboratory, Madison, WI.

3. Clapp, V. W. 1982. Lumber recovery: how does your mill's performance rate? Forest Industries 109(3): 26-27.

4. Higgs, M. 1989. Economic advantages of saw management. Forest Industries 166(5): T17-T19.

5. Mote, C. D.; Nieh, L. T. 1973. On the foundation of circular saw stability theory. Wood and Fiber 5(2): 160-169.

6. Dugdale, D. S. 1966. Theory of circular saw tensioning. International Journal of Production Research 4: 237-248.

7. Schajer, G. S. 1984. Understanding saw tensioning. Holz als Roh-und Werkstoff 42: 425-430.

8. Quelch, P. S. 1970. Armstrong Sawfiler's Handbook, 2nd Edition. Armstrong Manufacturing Co., Portland, OR. pp. 1-6 and pp. 75-85.

9. Stephenson, E.; Plank, D. 1972. Circular Saws. Thomas Robinson and Sons Ltd., Rochdale, England. pp. 68-94.

10. Umetsu, J.; Noguchi, M.; Matsumoto, I. 1987. A new technique of tensioning circular saws using shot peening. Mokuzai Gakkaishi 33(10): 818-820.

11. Mote, C. D.; Schajer, G. S.; Holoyen, S. 1981. Circular saw vibration control by induction of thermal membrane stresses. Journal of Engineering for Industry 103(2): 81-89.

12. Huber, H. 1991. Straightening and tensioning of circular saws by means of laser. Proceedings of the Tenth International Wood Machining Seminar. Forest Products Laboratory, Richmond, CA.

13. Szymani, R.; Mote, C .D. 1977. Circular saw stiffness as a measure of tension. Forest Products Journal 27(3): 28-32.

14. Mote, C. D.; Szymani, R. 1977. Principal developments in thin circular saw vibration and control research. Part I: Vibration of circular saws. Holz als Roh-und Werkstoff 35: 189-196.

15. Szymani, R.; Mote, C .D. 1974. A review of residual stress and tensioning in circular saws. Wood Science and Technology 8: 148-161.

16. Schajer, G. S. 1992. North American techniques for circular saw tensioning and levelling: Practical measurement methods. Holz als Roh-und Werkstoff 50: 111-116.

17. Szymani, R.; Trinchera, L.; Turner, J. 1987. Use and maintenance of thin circular saws at California Cedar Products Company. Holz als Roh-und Werkstoff 45: 319-322.

18. Schajer, G. S. 1981. Analysis of roller induced residual stresses in circular discs and their effect on disc vibration. PhD Thesis, University of California, Berkeley, CA.

19. Schajer, G. S. 1985. CSAW guided circular saw vibration and stability program, version 2.4. Science and Process Control Unit, Weyerhaeuser Technology Center, Tacoma, WA.

20. Taylor, J.; Hutton, S. G. 1990. The automation of bandsaw roll tensioning. Phase I: Roll tensioning stresses and performance. Project No. 12-71-K-404, Forintek Canada Corp., Vancouver, B.C.

21. Foschi, R. O. 1975. The light-gap technique as a tool for measuring residual stresses in bandsaw blades. Wood Science and Technology 9: 243-255.

22. Conway, H. D.; Nickola, W. E. 1965. Anticlastic action of flat sheets in bending. Experimental Mechanics 5(4): 115-119.

23. Leissa, A. W. 1969. Vibration of Plates. Technical Information Division, National Aeronautics and Space Administration, Washington DC. pp. 53-58.

24. Tse, F. S.; Morse, I. E.; Hinkle, R. T. 1978. Mechanical Vibrations, Theory and Applications, Second Edition. Allyn and Bacon Inc., Boston, MA. pp. 288-289.

25. Iyengar, N. G. R. 1988. Structural Stability of Columns and Plates. Ellis Horwood Ltd., Chichester, England. pp. 163-178.

26. Lister, P. F.; Schajer, G. S. 1991. The effectiveness of the light-gap and frequency measurement methods for evaluating saw tensioning. Proceedings of the Tenth International Wood Machining Seminar. Forest Products Laboratory, Richmond, CA.